



The evaluation of American options in a stochastic volatility model with jumps: An efficient finite element approach

Luca Vincenzo Ballestra^{a,1}, Carlo Sgarra^{b,*}

^a Dipartimento di Scienze Sociali “D. Serrani”, Università Politecnica delle Marche, Piazza Martelli 8, 60121 Ancona, Italy

^b Dipartimento di Matematica “F. Brioschi”, Politecnico di Milano, Piazza Leonardo Da Vinci 32, 20133 Milano, Italy

ARTICLE INFO

Article history:

Received 1 March 2010

Received in revised form 9 June 2010

Accepted 22 June 2010

Keywords:

Option pricing

Stochastic volatility

Lévy processes

Finite elements

ABSTRACT

We consider the problem of pricing American options in the framework of a well-known stochastic volatility model with jumps, the Bates model. According to this model the asset price is described by a jump-diffusion stochastic differential equation in which the jump term consists of a Lévy process of compound Poisson type, while the volatility is modeled as a CIR-type process correlated with the asset price. Pricing American options under the Bates model requires us to solve a partial integro-differential equation with the final condition and boundary conditions prescribed on a free boundary. In this paper a numerical method for solving such a problem is proposed. In particular, first of all, using a Richardson extrapolation technique, the problem is reduced to a problem with fixed boundary. Then the problem obtained is solved using an ad hoc finite element method which efficiently combines an implicit/explicit time stepping, an operator splitting technique, and a non-uniform mesh of right-angled triangles. Numerical experiments are presented showing that the option pricing algorithm developed in this paper is extremely accurate and fast. In particular it is significantly more efficient than other numerical methods that have recently been proposed for pricing American options under the Bates model.

© 2010 Elsevier Ltd. All rights reserved.

1. Introduction

The Black–Scholes model [1], originally introduced in 1973, is still nowadays widely used to price financial derivatives, due to its simplicity and analytical tractability. However, according to several empirical studies, it does not give a correct description of the financial market behavior. In particular, the probability distribution of realized asset returns often exhibits features that are not taken into account by the Black–Scholes model: heavy tails, volatility clustering, and aggregational Gaussianity [2] are some peculiarities that cannot be explained on the basis of the log-normal assumption on which the Black–Scholes model rests. Moreover the so-called volatility smile [2] is another relevant effect that cannot be predicted on the basis of the Black–Scholes model.

Several different approaches have been exploited in order to give a more satisfactory description of financial markets, but the main contributions in this direction can be grouped into two different classes of models, the models with stochastic volatility (or stochastic volatility models) and the models with jumps. An extended literature is available on both these approaches: in particular, they give a more realistic description of the price evolution in financial markets, however, if considered separately, they perform significantly well only in special circumstances. For example, while models with jumps can successfully reproduce the volatility smiles on short term maturity ranges, stochastic volatility models give a better description of the same phenomenon on long maturity terms. This has naturally led to the introduction of more complex,

* Corresponding author. Tel.: +39 02 23994570; fax: +39 02 23994621.

E-mail addresses: l.v.ballestra@univpm.it (L.V. Ballestra), carlo.sgarra@polimi.it (C. Sgarra).

¹ Tel.: +39 071 2207251; fax: +39 071 2207150.

but more realistic models in which both features of stochastic volatility and jumps can be present. The three more popular models in which the integration of jumps and stochastic volatility has been performed are the BNS model, introduced by Barndorff-Nielsen and Shephard [3,4], the model introduced by Bates [5], and the time-changed Lévy models introduced by Carr et al. [6]. While in the former the volatility dynamics is driven by a positive Lévy process correlated with the jump process driving the log-asset price, in the latter the volatility dynamics is governed by a time-changed Lévy process. In the present work we shall concentrate on the second model that we have just mentioned, the Bates model, in which a Merton jump-diffusion model [7] is combined with a stochastic volatility model of the Heston type [8]. As Cont and Tankov [2] have pointed out, the time-changed Lévy models can fit observed option prices much better than the BNS model: in the BNS model, in fact, the implied volatility patterns are restricted by the requirement that the same correlation parameter characterizes the returns for both short and long maturities; on the other hand the capabilities of the Bates model for fitting realized market prices are comparable to those of the time-changed Lévy processes, and “Thus the Bates model appears to be at the same time the simplest and the most flexible of the model” [2] (p. 495).

In the financial literature several numerical approaches have been proposed for pricing options under both models with stochastic volatility and models with jumps. In particular, in the case of models with jumps, we mention the paper by Matache et al. [9], where a finite element method is developed, the papers by Andersen and Andreasen [10], by Cont and Voltchkova [11], by d'Halluin et al. [12,13], and by Clift and Forsyth [14], where finite difference schemes are presented, and the papers by Fang and Oosterlee [15,16], where a numerical method based on the characteristic function is proposed. Moreover, as regards the case of stochastic volatility models, finite element methods are presented in Achdou and Tchou [17] and in Hilber et al. [18], whereas finite difference schemes are proposed in a number of papers, among which we mention those by Clarke and Parrot [19] and by Ikonen and Toivanen [20–22]. We also mention that numerical simulations of a stochastic volatility model are also presented in the aforementioned paper [15].

In contrast, as far as numerical techniques for the Bates model are concerned, very few works are available. In particular, a finite element method for European Call and Put options has been developed in [23], in order to establish a basis for pricing more complex exotic products. Instead, in the case of American options, a numerical method has recently been presented by Chiarella et al. [24]. In particular, in this latter work, a finite difference scheme and the method of lines are used to reduce the American option pricing problem to a system of second-order ordinary differential equations. However the results obtained reveal that such an approach is not particularly efficient. This is mainly due to the fact that the ordinary differential problem obtained is still a free boundary problem and thus must be solved using a time-consuming fixed-point iteration procedure.

A numerical method for pricing American options under the Bates model has also been proposed by Toivanen in [25], where a finite difference scheme coupled with a componentwise splitting technique is employed. However, according to the results presented, this numerical scheme is not particularly fast. In fact the American problem is solved as a linear complementarity problem, and then a time-consuming fixed-point iteration procedure must be performed at each time step. Moreover, the componentwise splitting technique employed in [25] requires a special treatment of the mixed second-order derivatives, which may cause some loss of accuracy, and imposes severe restrictions on the choice of the grid step sizes when a non-uniform mesh is employed (see [21,22]). Finally it is worth noticing that in [24] Chiarella et al. test the componentwise splitting employed in [25], and highlight serious accuracy and stability issues.

Finally an analytical approach to pricing American options under the Bates model has also been proposed by Cheang et al. [26], who prove that the option price could be obtained as the solution of a linked system of integral equations. However, such a system appears to be extremely complex from the mathematical standpoint, and, as acknowledged in [26], also very onerous to solve. In this respect it should be noted that in [26] a numerical method for solving the system of integral equations obtained is not presented.

In the present paper we propose a highly efficient numerical method for pricing American options on an underlying described by the Bates model. We start by noticing that this problem poses severe analytical and approximation difficulties: first of all the early exercise feature strongly complicates the problem from the mathematical standpoint and makes it impracticable to use methods based on the knowledge of the characteristic function (see [27]), which instead can be successfully employed in the European case. Furthermore the fact that the option payoff has discontinuous derivative may produce severe losses of accuracy if a finite difference/finite element discretization is applied. Finally a fully implicit time discretization scheme, that would guarantee unconditional stability, can hardly be employed. In fact such an approach, due to the presence of the non-local integral operator, leads to a dense linear system of equations, whose numerical approximation would be very time-consuming and requires large memory storage.

Note that the jump-integral term has the form of a convolution product, and hence could be quickly evaluated using a numerical quadrature rule based on the fast Fourier transform. Such an approach, pioneered by Andersen and Andreasen [10], and followed, for instance, by Clift and Forsyth [14], by d'Halluin et al. [12], and by d'Halluin et al. [28], would allow one to compute the jump-integral term with $O(N_S \log_2 N_S)$ floating point operations, against the N_S^2 floating point operations required by conventional integration rules (N_S being the number of grid prices). However, as reported in [28], the use of the fast Fourier transform introduces additional localization and interpolation error, especially if it is employed in conjunction with a non-uniform spatial mesh, so the discretization of the integral operator must be performed on a mesh which is finer than the mesh used for the discretization of the differential operators. Furthermore, as explained in [14,12,28], the use of the fast Fourier transform requires an iterative solution procedure (unless a fully explicit time stepping is employed), so the calculation of the jump-integral term must be repeated a certain number of times at each time step (roughly three times; see [14]). Therefore, given also that, in practical applications, the number of grid prices N_S

is limited, for computational reasons, to values of order 10^2 , the advantage of using the fast Fourier transform appears to be relatively small.

The numerical method proposed in the present paper for pricing American options under the Bates model is as follows. First of all the American option price is obtained by Richardson extrapolation of the prices of two Bermudan options. This is a very efficient approach for taking into account the possibility of early exercise. In fact, in contrast to other methods used to price American options, such as the linear complementarity method (see for example [29,22,30]), or the penalty method (see [31,13]), the Richardson extrapolation technique does not require one to perform a fixed-point iteration procedure. The Bermudan option pricing problems obtained are solved using an implicit/explicit time stepping and a finite element method based on a non-uniform (stretched) mesh of right-angled triangles. This kind of discretization, employed in conjunction with an operator splitting technique, allows one to obtain linear systems of equations that can be solved very efficiently. In particular, the use of a non-uniform mesh allows us to use a limited number of grid prices and grid variances, so the jump-integral term can be evaluated quickly. We want to mention explicitly that one of the main ingredients for forming this new method, the so-called “grid stretching technique”, suitable for dealing with the non-smooth payoff, has already been applied in a different model framework by Clarke and Parrot [19] and by Oosterlee et al. [32].

Several numerical experiments are presented showing that the numerical method proposed in this paper is very accurate and fast. In fact, if the simulations are carried out on a computer with a Pentium Dual Core E 2140 Processor 1.6 GHz 2 GB RAM, the American option price, the hedge parameters Δ and Γ , and the early exercise boundary are obtained with relative errors of order 10^{-4} or smaller in a time equal to or smaller than 16.3 s. In addition, the computer time necessary for evaluating the jump-integral term and the computer time necessary for evaluating (all) the differential terms are approximately the same, which indicates that the discretization of the jump-integral operator has been carried out efficiently. Furthermore, the experiments performed also reveal that the numerical method proposed in this paper is considerably faster than the numerical method presented in [24] and in [25].

We point out that the numerical tools employed in this paper (the Richardson extrapolation, the implicit/explicit time stepping, the operator splitting, the finite element method, the non-uniform mesh), considered separately, are not new. Nevertheless, to the best of our knowledge, an approach that puts all these techniques together has never been proposed in mathematical finance to solve complex models and it appears to be interesting in itself. In fact it is *only* thanks to the *appropriate* combination of *all* the above techniques that an accurate and computationally fast approximation of the Bates model can be obtained. To put this differently, a relevant contribution of this paper is to show how relatively simple techniques can be suitably combined to produce a highly efficient numerical method for pricing American options under the Bates model. In particular the method obtained performs significantly better than other methods that have been recently proposed for solving the same kind of problem. Furthermore the numerical approach proposed in this paper could also be easily extended to price other kinds of derivatives, such as barrier options, volatility derivatives, and even more exotic products.

The paper is organized as follows: in Section 2 we recall the basic facts about the Bates model, while in Section 3 we present the final-free boundary partial integro-differential problem that allows us to price American options; in Section 4 we describe the finite element method used to solve the problem presented in Section 3; in Section 5 we expose and discuss the numerical results obtained, whereas in Section 6 some conclusions are drawn.

2. The Bates model

As the main purpose of this paper is to provide an accurate and efficient method for evaluating American options, we briefly recall how these contracts are defined. While European Call options are contracts granting the holder the right, but not the obligation, to buy an asset with value S at a specified time T (the “maturity” of the option, or its exercise date) at a specified price K (the exercise price or “strike” of the option), American Call options give the holder the much stronger right to buy the asset at the specified price K at any time before the maturity T . European and American Put options are defined similarly as contracts granting the holder the right, but not the obligation, to sell an asset at a specified price at a specified date (in the European case) or before a specified date (in the American case).

The valuation of American contracts provides greater challenges than the valuation of European contracts since, as we shall see in the next section, it amounts to solving a free boundary problem for a partial integro-differential equation. The values of the Call and Put options at the exercise date, their “payoffs”, are then respectively provided by the following expressions:

$$\begin{aligned} C &= \max(S - K, 0), \\ P &= \max(K - S, 0). \end{aligned}$$

The Bates model combines a stochastic volatility dynamics with jumps in the asset price. While the former is described using a CIR-type stochastic differential equation with mean reversion, the latter is modeled by means of a compound Poisson process (CIR is an abbreviation for three author names: Cox, Ingersoll and Ross, who introduced this model to describe the short interest rates dynamics [33]; in the probabilistic literature it is better known as the Feller process).

In the Bates model the asset price evolution is then given by

$$S_t = S_0 e^{X_t}, \quad (1)$$

where the log-return X and its volatility Y satisfy the following initial value stochastic differential problems:

$$dX_t = \left(\alpha - \frac{1}{2} Y_t \right) dt + \sqrt{Y_t} dW_t^1 + dZ_t, \quad X_0 = 0. \quad (2)$$

$$dY_t = \xi(\eta - Y_t)dt + \theta\sqrt{Y_t}dW_t^2, \quad Y_0 = y_0, \quad (3)$$

where $y_0 > 0$, and $\alpha, \xi, \eta, \theta$ are parameters such that

$$\alpha \in \mathbb{R}, \quad \xi \geq 0, \quad \eta \geq 0, \quad \theta \geq 0. \quad (4)$$

While the α parameter measures the “drift” of the log-return process X , the parameters ξ and η are the mean-reversion rate and the long term mean of the Y process, respectively; the parameter θ is the diffusion coefficient of the Feller process describing the dynamics of Y , and is sometimes referred to as “the volatility of the volatility” of the model. Moreover, in (2) and (3) W^1 and W^2 are Wiener standard processes having constant correlation ρ , and Z is a compound Poisson process.

The process X takes values on the whole real domain. Instead, as far as the process Y is concerned, it can be shown that, if the following condition is satisfied:

$$\theta^2 < 2\xi\eta, \quad (5)$$

then the volatility process Y remains strictly positive (see [34]).

The process Z is a Levy processes with finite activity. Thus, for the reader's convenience, the basic facts about the Levy processes are recalled in the following. In particular we will give a complete characterization of the dynamics of the asset price process S (Eq. (10)). For an exhaustive description of the Levy processes the reader is referred to [35].

For a Lévy process the cumulant function $\kappa(z)$ is defined as follows:

$$\kappa(z) := \frac{1}{t} \log E \left[e^{izZ_t} \right]. \quad (6)$$

Since the Lévy–Khintchine representation holds, the cumulant function can be written as follows:

$$\kappa(z) = -\frac{1}{2}Az^2 + i\beta z + \int_{-\infty}^{+\infty} (e^{izx} - 1 - izxh(x))U(dx), \quad (7)$$

where β is the drift of the process, A the quadratic variation component, h the truncation function, and $U(dx)$ is the Lévy measure of Z .

The choices of the truncation function h and the drift coefficient β are strongly interconnected. A usual choice for h is the following: $h(x) := \mathbf{1}_{|x| \leq 1}$. Moreover, since in the Bates model Z is a compound Poisson without diffusion component, we have $A = 0$. We assume moreover $E[Z_1^2] < \infty$; these statements allow us to rewrite relation (7) as follows:

$$\kappa(z) = i\zeta z + \int_{-\infty}^{+\infty} (e^{izx} - 1 - izx)U(dx), \quad (8)$$

where $\zeta = E[Z_1]$, and its relation with β is the following: $\zeta = \beta + \int_{|x| \geq 1} xU(dx)$.

We denote by $\mu(dx, dt)$ the jump measure of Z and by $\nu(dt, dx)$ its predictable compensator. Moreover we have $\nu(dx, dt) = U(dx)dt$. By the Lévy–Itô decomposition specified for compound Poisson processes, we can write then

$$Z_t = \zeta t + \int_0^t \int_{-\infty}^{+\infty} x(\mu - \nu)(dx, ds). \quad (9)$$

Lemma 1. *The dynamics of the asset price process is given by*

$$dS_t = (\alpha + \kappa(1))S_{t-}dt + S_{t-}\sqrt{Y_t}dW_t^1 + \int_{-\infty}^{+\infty} S_{t-}(e^x - 1)(\mu - \nu)(dx, dt). \quad (10)$$

In particular if

$$\alpha + \kappa(1) = 0, \quad (11)$$

then the process S is a local martingale.

Proof. This follows immediately from Itô's formula for general semimartingales applied to the asset price model with the dynamics described by (1) and (2), and from the Lévy–Itô representation formula for compound Poisson processes (9). \square

The lemma stated above provides a complete characterization of the dynamics of the asset price through the semimartingale characteristics (see [36]) of the stochastic process S : the first term in the sum is the drift, the second is the quadratic variation component, the third is specified as an integral with respect to a (compensated) jump measure.

Remark 2. In the original model proposed by Bates [5], the process Z is the compound Poisson process:

$$Z_t = \sum_{i=1}^{N_t} J_i, \quad (12)$$

where N is a standard Poisson process with intensity $\lambda > 0$ and $(J_i), i = 1, 2, 3, \dots$, are independent random variables, all having a normal distribution with mean γ and standard deviation δ , where $\gamma = \ln(1 + \kappa(1)/\lambda) - \delta^2/2$. In such a case the Lévy measure of Z is given by

$$U(dx) = \frac{\lambda}{\delta\sqrt{2\pi}} \exp\left[-\frac{(x-\gamma)^2}{2\delta^2}\right], \quad (13)$$

and the cumulant function of Z takes the form

$$\kappa(z) = \lambda(e^{\gamma z + \delta^2 z^2/2} - 1). \quad (14)$$

Remark 3. If $Z = 0$, then we obtain the Heston stochastic volatility model [8]. If $\theta = 0$ and $Y_t = \eta$ we obtain the Merton jump-diffusion model [7]. Consequently we might consider the Bates model as an extension of a Merton model to the case of stochastic volatility, or as an extension of the Heston stochastic volatility model to the case of jumps in the asset prices.

3. The partial integro-differential approach

Following a usual derivation based on Itô's lemma and the no arbitrage requirement, we obtain the following partial integro-differential equation for the price of a European Call option:

$$\begin{aligned} \frac{\partial C}{\partial t} + (r - q - \kappa(1))S \frac{\partial C}{\partial S} + \frac{1}{2}yS^2 \frac{\partial^2 C}{\partial S^2} + [\xi(\eta - y) - \pi] \frac{\partial C}{\partial y} + \frac{1}{2}\theta^2 y \frac{\partial^2 C}{\partial y^2} \\ + \rho\theta yS \frac{\partial^2 C}{\partial y \partial S} + \lambda \int_{-\infty}^{+\infty} C(Se^x, y, t)W(dx) = (r + \lambda)C, \end{aligned} \quad (15)$$

with final condition at $t = T$

$$C(S, y, T) = \max[S - K, 0], \quad (16)$$

and boundary conditions

$$C(0, y, t) = 0, \quad C(S, y, t) = S - K, \text{ as } S \rightarrow +\infty, \quad (17)$$

where T is the option's maturity, K is the option's exercise price, r is the interest rate, and q is the dividend yield. Note that both r and q are assumed to be constant; however generalizations to more complex (e.g. time-varying) interest rate and dividend structures are straightforward. Moreover, for the sake of simplicity, and following a common approach, in Eq. (15) the market price of volatility risk and the market price of jump risk are both set to zero. This assumption implies that the drift coefficient α in Eq. (2) is considered equal to $r - q$, and that the jump distribution remains unchanged under the risk-neutral measure [2]. In Eq. (15) $W(dx)$ denotes the probability density function of the jumps in the log-returns, and is related to the Levy measure $U(dx)$ as follows:

$$W(dx) = \frac{U(dx)}{\lambda}, \quad (18)$$

which, together with (13), implies

$$W(dx) = \frac{1}{\delta\sqrt{2\pi}} \exp\left[-\frac{(x-\gamma)^2}{2\delta^2}\right]. \quad (19)$$

Finally from Remark 2 we have

$$\kappa(1) = \lambda(e^{\gamma + \delta^2/2} - 1). \quad (20)$$

When pricing American Call options the above final-boundary value partial integro-differential problem must be suitably modified in order to take into account the possibility of early exercise. Let $S_f(y, t)$ denote the value of the underlying asset price at which the American option is exercised (this value varies as a function of the current time and volatility). Since the price of an American option can never fall below the payoff, a “value matching” condition must be prescribed on $S_f(y, t)$. To be precise, the boundary conditions (17) must be replaced as follows:

$$C(0, y, t) = 0, \quad C(S_f(y, t), y, t) = S_f(y, t) - K. \quad (21)$$

Furthermore the function $S_f(y, t)$ must satisfy the “smooth pasting” conditions (see [24]):

$$\lim_{s \rightarrow S_f(y, t)} \frac{\partial C}{\partial S} = 1, \quad \lim_{s \rightarrow S_f(y, t)} \frac{\partial C}{\partial y} = 0. \quad (22)$$

In particular, since the first of the boundary conditions (21) is assigned on $S_f(y, t)$, which is not known a priori, the partial integro-differential problem that must be solved to price American options under the Bates model, i.e. the problem (15), (16), (21), (22), is a free boundary problem.

A detailed analytical investigation of the early exercise boundary has been carried out by, for example, Sevcovic [37]. In particular in this work, dealing with linear and non-linear Black–Scholes equations, a method for transforming the American problem to a fixed-boundary problem is proposed. However the extension of this very recently developed technique to models with stochastic volatility and/or to models with jumps does not appear to be straightforward.

Remark 4. Looking at the problem (15), (16), (21), (22), we may note that no boundary condition has been prescribed at $y = 0$ and $y \rightarrow +\infty$. In fact the partial integro-differential equation (15) is singular at both $y = 0$ and $y \rightarrow +\infty$, and it is not clear which boundary conditions to apply on these boundaries. The most insightful result on this subject has been obtained by Feller [34], who shows that at $y = 0$ a boundary condition should be imposed only if the condition (5) is not satisfied. However, to the best of our knowledge, a thorough investigation on the boundary conditions at $y = 0$ and $y \rightarrow +\infty$ is still lacking. In this paper following a common approach (see for instance [24]) we will circumvent the problem by extrapolating the solution at $y = 0$ and $y \rightarrow +\infty$ from the numerical solution obtained in the interior of the (S, y) computational domain (see Section 4).

A final-boundary value partial integro-differential problem analogous to problem (15), (16), (21), (22) can be obtained also for American Put options. To be precise, the price of an American Put option must satisfy the partial integro-differential equation

$$\frac{\partial P}{\partial t} + (r - q - \kappa(1))S \frac{\partial P}{\partial S} + \frac{1}{2}yS^2 \frac{\partial^2 P}{\partial S^2} + [\xi(\eta - y) - \pi] \frac{\partial P}{\partial y} + \frac{1}{2}\theta^2 y \frac{\partial^2 P}{\partial y^2} \quad (23)$$

$$+ \rho\theta yS \frac{\partial^2 P}{\partial y \partial S} + \lambda \int_{-\infty}^{+\infty} P(Se^x, y, t)W(dx) = (r + \lambda)P, \quad (24)$$

with final condition

$$P(S_T, y_T, T) = \max[K - S_T, 0], \quad (25)$$

and boundary conditions

$$P(S_f(y, t), y, t) = K - S_f(y, t), \quad P(S, y, t) = 0, \text{ as } S \rightarrow +\infty, \quad (26)$$

$$\lim_{S \rightarrow S_f(y, t)} \frac{\partial P}{\partial S} = -1, \quad \lim_{S \rightarrow S_f(y, t)} \frac{\partial P}{\partial y} = 0. \quad (27)$$

We point out that in the Bates model, as in other affine stochastic volatility models with and without jumps, it is possible to obtain the characteristic function of the log-asset price process in closed form. This has been done by Bates [5], although a detailed derivation is also provided in [2]; when the jumps are log-normally distributed, the characteristic function of the log-asset price process has the following expression:

$$\begin{aligned} \Phi_t(u) = & \exp \left[t\lambda e^{-\delta^2 u^2/2 + i(\ln(1+\kappa(1)/\lambda) - \delta^2/2)u} - 1 \right] \\ & \times \frac{\exp \left[\frac{\xi\eta t(\xi - i\rho\theta u)}{\theta^2} + iut(r - q - \kappa(1)) \right]}{\left[\cosh \frac{\varepsilon t}{2} + \frac{\xi - i\rho\theta u}{\varepsilon} \sinh \frac{\varepsilon t}{2} \right]^{2\xi\eta/\theta^2}} \exp \left[-\frac{(u^2 + iu)y_0}{\varepsilon \coth \frac{\varepsilon t}{2} + \xi - i\rho\theta u} \right], \end{aligned} \quad (28)$$

where

$$\varepsilon = \sqrt{\theta^2(u^2 + iu) + (\xi - i\rho\theta u)^2}. \quad (29)$$

Once the characteristic function of the log-asset price process is available in closed form, then European Call and Put options can be priced using, for example, a technique based on the fast Fourier transform; see [27] and [15]. Unfortunately such an approach cannot be extended to the case of American options in a straightforward manner. For example, in the case of constant volatility, efficient methods for pricing American options based on the characteristic function have been proposed by Fang and Oosterlee [16]. This approach requires, at each time step, the numerical approximation of some one-dimensional integrals (integrals (17) and (18) in [16]), whose domains depend on the unknown location of the option's early exercise boundary. In particular, in [16], the early exercise boundary is given by a single price, due to the constant volatility assumption, and is obtained using a Newton iteration procedure. Now, if the method of Fang and Oosterlee is used for pricing American options under the Bates model with stochastic volatility, then the integrals to be computed at each time step are double integrals, and, in addition, their domains are defined by an unknown line in the (S, y) plane (the early exercise boundary). It is then clear how this introduces severe complications, in terms of both accuracy and computational efficiency, so the approach based on the characteristic function does not appear to be particularly suitable for pricing American options with stochastic volatility.

It should also be observed that methods based on the characteristic function offer less flexibility than finite difference and finite element techniques. In fact, while the latter can handle a broad range of situations, the former are only applicable in those cases where the characteristic function is available in closed form (this does not happen, for example, when the interest rate or the jump's arrival intensity is assumed to be time dependent).

4. The numerical method

For ease of exposition we will limit our attention to the case of American Call options. However the reader will note that the numerical method presented in this section can be used with little modifications also to price American Put options (an American Put option will be considered in one of the test cases presented in Section 5). Then our starting point is Eq. (15), which it is convenient to recast in the conservative form

$$\begin{aligned} \frac{\partial C}{\partial t} + \frac{1}{2} \frac{\partial}{\partial S} \left(y S^2 \frac{\partial C}{\partial S} \right) + \frac{1}{2} \frac{\partial}{\partial y} \left(\theta^2 y \frac{\partial C}{\partial y} \right) + \frac{1}{2} \rho \theta \frac{\partial}{\partial S} \left(y S \frac{\partial C}{\partial y} \right) \\ + \frac{1}{2} \rho \theta \frac{\partial}{\partial y} \left(y S \frac{\partial C}{\partial S} \right) + \left(r - q - \lambda \kappa(1) - y - \frac{1}{2} \rho \theta \right) S \frac{\partial C}{\partial S} \\ + \left[\xi(\eta - y) - \frac{1}{2} \theta^2 - \frac{1}{2} \rho \theta y \right] \frac{\partial C}{\partial y} + \lambda \int_{-\infty}^{+\infty} C(\text{Se}^x, y, t) W(dx) = (r + \lambda)C. \end{aligned} \quad (30)$$

Let us rewrite Eq. (30) in the compact form

$$\frac{\partial C}{\partial t} + \mathcal{L}C = (r + \lambda)C, \quad (31)$$

where

$$\mathcal{L} = \mathcal{L}_1 + \mathcal{L}_2 + \mathcal{L}_3 + \mathcal{L}_4 + \mathcal{L}_5 + \mathcal{L}_6, \quad (32)$$

and

$$\mathcal{L}_1 C = \frac{1}{2} \frac{\partial}{\partial S} \left(y S^2 \frac{\partial C}{\partial S} \right), \quad (33)$$

$$\mathcal{L}_2 C = \frac{1}{2} \frac{\partial}{\partial y} \left(\theta^2 y \frac{\partial C}{\partial y} \right), \quad (34)$$

$$\mathcal{L}_3 C = \frac{1}{2} \rho \theta \frac{\partial}{\partial S} \left(y S \frac{\partial C}{\partial y} \right) + \frac{1}{2} \rho \theta \frac{\partial}{\partial y} \left(y S \frac{\partial C}{\partial S} \right), \quad (35)$$

$$\mathcal{L}_4 C = \left(r - q - \lambda \kappa(1) - y - \frac{1}{2} \rho \theta \right) S \frac{\partial C}{\partial S}, \quad (36)$$

$$\mathcal{L}_5 C = \left[\xi(\eta - y) - \frac{1}{2} \theta^2 - \frac{1}{2} \rho \theta y \right] \frac{\partial C}{\partial y}, \quad (37)$$

$$\mathcal{L}_6 C = \lambda \int_{-\infty}^{+\infty} C(\text{Se}^x, y, t) W(dx). \quad (38)$$

For the sake of clarity this section is divided into four subsections. In Section 4.1 Eq. (31) is discretized in time. In particular it is shown how to take into account the early exercise feature. In Section 4.2 the finite element approximation of the differential operators \mathcal{L}_1 , \mathcal{L}_2 , \mathcal{L}_3 , \mathcal{L}_4 and \mathcal{L}_5 is carried out. Finally in Section 4.3 the discretization of the integral operator \mathcal{L}_6 is performed.

4.1. Time discretization

Richardson extrapolation. The option price is computed by Richardson extrapolation of the prices of two Bermudan options. The computational advantages of such an approach have been assessed, for instance, by Lord et al. in [38], who claim that American options are priced “efficiently by applying Richardson extrapolation to the prices of Bermudan options”. In essence the Richardson approximation allows one to reduce the free boundary problem (15), (16), (22) to a problem with fixed boundary, which is much simpler to solve than the original free boundary problem. As a consequence, the Richardson extrapolation is computationally faster than other methods used to price American options, such as the linear complementarity method (see for example [29,22,30]), or the penalty method (see [31,13]), which require one to perform a fixed-point iteration at each time step. Furthermore, in Section 5 we will show by direct numerical simulation that the Richardson extrapolation method, when it is used to price American options under the Bates model, is not only computationally fast, but also very accurate.

Let us consider, in the interval $[0, T]$, $N_t + 1$ equally spaced time levels $t_0 = 0, t_1, t_2, \dots, t_{N_t} = T$. Moreover let us define $\Delta t = t_k - t_{k-1}$, $k = 1, 2, \dots, N_t$. Let $C_{N_t}(S, y, t)$ denote the price of a Bermudan option with maturity T and exercise dates t_k , $k = 0, 1, \dots, N_t$. The Bermudan option price $C_{N_t}(S, y, t)$ is obtained using the following recursion procedure. First of all set $k := N_t$ and define

$$\Psi_{N_t}(S, y, t_k) = \max[S - K, 0]. \quad (39)$$

Then solve the final-boundary value partial differential problem

$$\frac{\partial C_{N_t}}{\partial t} + \mathcal{L}C_{N_t} = (r + \lambda)C_{N_t}, \quad t \in [t_{k-1}, t_k], \quad (40)$$

$$C_{N_t}(0, y, t) = 0, \quad C_{N_t}(S, y, t) = S - E \quad \text{as } S \rightarrow +\infty, \quad (41)$$

$$C_{N_t}(S, y, t_k) = \Psi_{N_t}(S, y, t_k). \quad (42)$$

Then define

$$\Psi_{N_t}(S, y, t_{k-1}) = \max[C_{N_t}(S, y, t_{k-1}), S - K], \quad (43)$$

and set

$$k := k - 1. \quad (44)$$

Repeat the cycle (40)–(44) and stop when $k := 0$.

The Bermudan option price $C_{N_t}(S, y, t)$ tends to become a fair approximation of the American option price $C(S, y, t)$ as the number of exercise dates N_t increases. In this paper the accuracy of $C_{N_t}(S, y, t)$ is enhanced by Richardson extrapolation:

$$C(S, y, t) \simeq 2C_{2N_t}(S, y, t) - C_{N_t}(S, y, t), \quad (45)$$

which is second-order accurate in time (see for instance [39]).

Implicit/explicit time stepping. Now we are going to describe the time discretization of the final-boundary value partial integro-differential problem (40)–(42). Let $U^k(S, y)$ denote a function approximating $C_{N_t}(S, y, t_k)$, $k = 0, 1, \dots, N_t - 1$, and let $\Psi^k(S, y)$ denote a function approximating $\Psi_{N_t}(S, y, t_k)$, $k = 1, 2, \dots, N_t$. Note that the subscript N_t has been removed from $U^k(S, y)$ and $\Psi^k(S, y)$ to keep the notation simple. According to (39) we set $\Psi^{N_t}(S, y) = \max[S - K, 0]$.

The problem (40)–(42) is discretized in time using the following one-step implicit/explicit finite difference scheme:

$$\frac{\Psi^k - U^{k-1}}{\Delta t} + \mathcal{L}_1 U^{k-1} + \mathcal{L}_2 U^{k-1} + \mathcal{L}_3 \Psi^k + \mathcal{L}_4 \Psi^k + \mathcal{L}_5 \Psi^k + \mathcal{L}_6 U^{k-1} = (r + \lambda)U^{k-1}, \quad (46)$$

$$U^{k-1}(0, y) = 0, \quad U^{k-1}(S, y) = S - E \quad \text{as } S \rightarrow +\infty, \quad (47)$$

which allows us to compute $U^{k-1}(S, y)$ given $\Psi^k(S, y)$. Note that the operator \mathcal{L}_1 , which contains the second-order derivative with respect to S , and the operator \mathcal{L}_2 , which contains the second-order derivative with respect to y , are treated implicitly. This choice is crucial for achieving stability also for large values of Δt . In contrast, the hyperbolic operators \mathcal{L}_3 , \mathcal{L}_4 and \mathcal{L}_5 are treated explicitly, in order to enhance the speed of the numerical calculations. This choice could potentially cause some numerical instability for large values of Δt when the weight of the hyperbolic terms \mathcal{L}_3 , \mathcal{L}_4 and \mathcal{L}_5 is bigger than that of the diffusive terms \mathcal{L}_1 and \mathcal{L}_2 . Nevertheless we have performed several numerical experiments where we have considered various kinds of Call and Put option contracts and we have used many different values for the parameters of the Bates model. In all these simulations (some of which are not reported in this paper) the numerical scheme (46) has always proven to be stable, and also for large values of Δt , which indicates that the Bates model is mainly dominated by diffusion.

Finally we note that in Eq. (46) the integral operator \mathcal{L}_6 is treated implicitly, in order to enhance stability. In the following we will show that this choice, thanks to an appropriate discretization of the jump-integral term, does not significantly increase the computer time necessary for the calculations.

Operator splitting. The final-boundary value partial integro-differential problem (46)–(47) is efficiently solved using an appropriate operator splitting technique. The operator splitting is actually a variant of the well-known ADI (alternating direction implicit) time stepping originally developed in Peaceman and Rachford [40]. In this paper we use the operator splitting rather than the ADI time stepping since: (1) the operator splitting is simpler to implement than the ADI time stepping (and also moderately less expensive); (2) the ADI time stepping leads to some loss of accuracy when it is applied to problems with mixed derivatives, as shown, for example, in [41].

Note also that the operator splitting is different from the componentwise splitting employed in [25]. Indeed, while the former acts directly on the differential operators $\mathcal{L}_1, \mathcal{L}_2, \dots, \mathcal{L}_6$, the latter acts (componentwise) on the matrices obtained from the discretization of the operators $\mathcal{L}_1, \mathcal{L}_2, \dots, \mathcal{L}_6$. In particular, according to the componentwise splitting employed in [25], the matrix obtained from the discretization of the mixed second-order derivatives is split into three submatrices. As shown in [25], this amounts to changing the coefficients of the diffusive operators in the partial integro-differential equation (15), and, according to numerical experiments carried out in [24], can cause serious accuracy and stability issues.

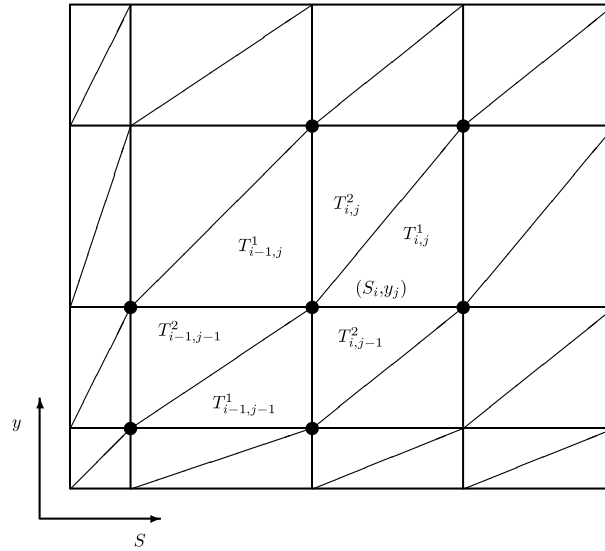


Fig. 1. Finite element mesh.

The operator splitting employed in this paper is as follows:

$$\frac{\Psi^k - V^{k-1}}{\Delta t} + \mathcal{L}_1 V^{k-1} + \mathcal{L}_3 \Psi^k + \mathcal{L}_4 \Psi^k + \mathcal{L}_5 \Psi^k = r V^{k-1}, \quad (48)$$

$$V^{k-1}(0, y) = 0, \quad V^{k-1}(S, y) = S - E \quad \text{as } S \rightarrow +\infty, \quad (49)$$

$$\frac{V^{k-1} - W^{k-1}}{\Delta t} + \mathcal{L}_2 W^{k-1} = 0, \quad (50)$$

$$W^{k-1}(0, y) = 0, \quad W^{k-1}(S, y) = S - E \quad \text{as } S \rightarrow +\infty, \quad (51)$$

$$\frac{W^{k-1} - U^{k-1}}{\Delta t} + \mathcal{L}_6 U^{k-1} = \lambda U^{k-1}, \quad (52)$$

$$U^{k-1}(0, y) = 0, \quad U^{k-1}(S, y) = S - E \quad \text{as } S \rightarrow +\infty. \quad (53)$$

That is, first of all the function $V^{k-1}(S, y)$ is obtained by solving (48)–(49), then the function $W^{k-1}(S, y)$ is obtained by solving (50)–(51), and finally the function $U^{k-1}(S, y)$ is obtained by solving (52)–(53). As will become clear in Sections 4.2 and 4.3 the splitting scheme (48)–(53) will allow us to obtain linear systems of equations that can be solved very quickly.

Remark 5. The scheme (48)–(53) is only first-order accurate in time (see for instance [42]). Nevertheless, the $O(\Delta t)$ component of the error is removed by the Richardson extrapolation (45), so the overall numerical method is second-order accurate in time. Note also that the Richardson extrapolation has the same order of accuracy as the more popular Crank–Nicholson scheme, provided that the solution has enough regularity (both of the methods require the existence of the second-order derivative of the solution with respect to time).

For the sake of simplicity, in the following, with reference to problems (48)–(49), (50)–(51), (52)–(53), we will write $\Psi^k(S, y)$, $V^{k-1}(S, y)$, $W^{k-1}(S, y)$, $U^{k-1}(S, y)$ instead of $\Psi(S, y)$, $V(S, y)$, $W(S, y)$, $U(S, y)$, respectively.

4.2. The finite element method

The partial differential problems (48)–(49) and (50)–(51) are solved using a finite element method based on a non-uniform (stretched) mesh of right-angled triangles (see Fig. 1). This approach, used in conjunction with the operator splitting technique (48)–(53), gives the following computational advantages:

- (1) the problems (48)–(49) and (50)–(51) are reduced to tridiagonal systems of linear equations, which can be solved very quickly;
- (2) the problem (52)–(53) can be solved very efficiently by exploiting the fact that $W^{k-1}(S, y)$ is obtained on a rectangular grid (see the next subsection);
- (3) the accuracy of the numerical solution can be improved by refining the mesh in certain regions of the $(S-y)$ plane. In particular, along the S -direction, it is crucial to use a refined mesh in a neighborhood of the strike price, where the

derivative of the option payoff is discontinuous. Moreover, along the y -direction, it is convenient to use a larger number of nodes in a neighborhood of y_0 , where the possible realizations of the stochastic variance are more likely to occur. Furthermore a non-uniform mesh allows us to use a limited number of grid prices, which is crucial to the efficiency of the overall numerical method. In fact, as shown later on in this section, the number of floating point operations necessary for computing the jump-integral operator is directly proportional to the square of the number of grid prices and to the number of grid variances used. Finally it should also be noticed that on a non-uniform mesh the finite element method is particularly suitable and, in the case of high mesh stretching, allows one to reach a better accuracy than the finite difference method (see for example [43,44]).

The finite element approximation is carried out as follows. First of all the spatial domain of the partial differential equation (48) and (50), which consists of the $[0, +\infty) \times [0, +\infty)$ quarter of the plane, is replaced with the finite domain $\Omega = [0, S_{\max}] \times [0, y_{\max}]$, where S_{\max} and y_{\max} are chosen sufficiently large (such that the possible realizations of S and y are contained in Ω with probability close to 1). Let us consider, in the interval $[0, S_{\max}]$, N_S nodes $S_1 = 0, S_2, S_3, \dots, S_{N_S} = S_{\max}$, and, in the interval $[0, y_{\max}]$, N_y nodes $y_1 = 0, y_2, y_3, \dots, y_{N_y} = y_{\max}$. Moreover let us define $\Delta S_i = S_{i+1} - S_i, i = 1, 2, \dots, N_S - 1$, and $\Delta y_j = y_{j+1} - y_j, j = 1, 2, \dots, N_y - 1$. Let $T_{i,j}^1$ denote the right-angled triangle with vertices $(S_i, y_j), (S_{i+1}, y_j), (S_{i+1}, y_{j+1})$ and let $T_{i,j}^2$ denote the right-angled triangle with vertices $(S_i, y_j), (S_{i+1}, y_{j+1}), (S_i, y_{j+1})$, $i = 1, 2, \dots, N_S - 1, j = 1, 2, \dots, N_y - 1$ (see Fig. 1). The finite element mesh \mathcal{T} is defined as the union of all the triangles $T_{i,j}^1, T_{i,j}^2, i = 1, 2, \dots, N_S - 1, j = 1, 2, \dots, N_y - 1$. Moreover let $\Omega_{i,j}$ denote the set of all the triangles with a vertex at (S_i, y_j) , that is $\Omega_{i,j} = \{T_{i-1,j-1}^1, T_{i,j-1}^1, T_{i,j}^1, T_{i,j}^2, T_{i-1,j}^1, T_{i-1,j-1}^2\}, i = 2, 3, \dots, N_S - 1, j = 2, 3, \dots, N_y - 1$ (see Fig. 1).

We want to approximate $V(S, y)$ and $W(S, y)$ using piecewise continuous linear functions. To be precise let $\phi_{i,j}(S, y)$, $i = 1, 2, \dots, N_S, j = 1, 2, \dots, N_y$, denote a set of trial functions defined as follows: $\phi_{i,j}(S, y)$ is continuous on Ω , piecewise linear on each triangle of \mathcal{T} , equal to 1 at the node (S_i, y_j) , and vanishes at all the other nodes, $i = 1, 2, \dots, N_S, j = 1, 2, \dots, N_y$. Note that the functions $\phi_{i,j}(S, y), i = 1, 2, \dots, N_S, j = 1, 2, \dots, N_y$, are the so-called *hat* functions that are often employed in finite element analysis (see [44,45]).

The functions $W(S, y), V(S, y)$ and $\Psi(S, y)$ are approximated as follows:

$$\Psi(S, y) \simeq \sum_{i=1}^{N_S} \sum_{j=1}^{N_y} \Psi_{i,j} \phi_{i,j}(S, y), \quad (54)$$

$$V(S, y) \simeq \sum_{i=1}^{N_S} \sum_{j=1}^{N_y} V_{i,j} \phi_{i,j}(S, y), \quad (55)$$

$$W(S, y) \simeq \sum_{i=1}^{N_S} \sum_{j=1}^{N_y} W_{i,j} \phi_{i,j}(S, y). \quad (56)$$

First of all let us show how to solve problem (48)–(49). We recall that $\Psi_{i,j}, i = 1, 2, \dots, N_S, j = 1, 2, \dots, N_y$, must be considered as known quantities, since they are computed at the previous iteration of the cycle (40)–(44).

We multiply Eq. (48) by $\phi_{i,j}(S, y)$ and integrate over $\Omega_{i,j}, i = 2, 3, \dots, N_S - 1, j = 2, 3, \dots, N_y - 1$, obtaining

$$\begin{aligned} (1 + r \Delta t) \int_{\Omega_{i,j}} V \phi_{i,j} dS dy - \Delta t \int_{\Omega_{i,j}} (\mathcal{L}_1 V) \phi_{i,j} dS dy &= \int_{\Omega_{i,j}} \Psi \phi_{i,j} dS dy \\ + \Delta t \int_{\Omega_{i,j}} (\mathcal{L}_3 \Psi) \phi_{i,j} dS dy + \Delta t \int_{\Omega_{i,j}} (\mathcal{L}_4 \Psi) \phi_{i,j} dS dy + \Delta t \int_{\Omega_{i,j}} (\mathcal{L}_5 \Psi) \phi_{i,j} dS dy, \\ i = 2, 3, \dots, N_S - 1, j = 2, 3, \dots, N_y - 1. \end{aligned} \quad (57)$$

Note that in (57) we are only considering the trial functions centered at the nodes that are internal points of Ω . In fact at the boundary, nodes $V(S, y)$ will be obtained by imposing suitable boundary conditions (see below).

Substituting (54) and (55) in (57), using relations (33), (35), (36), (37), and applying standard finite element techniques (see for instance [45]) the integrals appearing in (57) are approximated as follows:

$$\int_{\Omega_{i,j}} V \phi_{i,j} dS dy \simeq \frac{1}{6} |\Omega|_{i,j} V_{i,j}, \quad (58)$$

$$\int_{\Omega_{i,j}} \Psi \phi_{i,j} dS dy \simeq \frac{1}{6} |\Omega|_{i,j} \Psi_{i,j}, \quad (59)$$

$$\int_{\Omega_{i,j}} (\mathcal{L}_1 V) \phi_{i,j} dS dy \simeq \frac{1}{12} [a_{1,i,j}(V_{i+1,j} - V_{i,j}) - a_{2,i,j}(V_{i,j} - V_{i-1,j})], \quad (60)$$

$$\int_{\Omega_{i,j}} (\mathcal{L}_3 \Psi) \phi_{i,j} dSdy \simeq \frac{1}{12} [a_{3,i,j}(\Psi_{i-1,j-1} - \Psi_{i,j-1}) + a_{4,i,j}(\Psi_{i,j} - \Psi_{i+1,j}) + a_{5,i,j}(\Psi_{i+1,j+1} - \Psi_{i,j+1}) + a_{6,i,j}(\Psi_{i,j} - \Psi_{i-1,j}) + a_{4,i,j}(\Psi_{i,j} - \Psi_{i,j-1}) + a_{7,i,j}(\Psi_{i+1,j+1} - \Psi_{i+1,j}) + a_{6,i,j}(\Psi_{i,j} - \Psi_{i,j+1}) + a_{8,i,j}(\Psi_{i-1,j-1} - \Psi_{i-1,j})], \quad (61)$$

$$\int_{\Omega_{i,j}} (\mathcal{L}_4 \Psi) \phi_{i,j} dSdy \simeq \frac{1}{6} a_{9,i,j} [(\Delta y_{j-1} + \Delta y_j)(\Psi_{i+1,j} - \Psi_{i-1,j}) + \Delta y_j(\Psi_{i+1,j+1} - \Psi_{i,j+1}) + \Delta y_{j-1}(\Psi_{i,j-1} - \Psi_{i-1,j-1})], \quad (62)$$

$$\int_{\Omega_{i,j}} (\mathcal{L}_5 \Psi) \phi_{i,j} dSdy \simeq \frac{1}{6} a_{10,i,j} [(\Delta S_{i-1} + \Delta S_i)(\Psi_{i,j+1} - \Psi_{i,j-1}) + \Delta S_i(\Psi_{i+1,j+1} - \Psi_{i+1,j}) + \Delta S_{j-1}(\Psi_{i-1,j} - \Psi_{i-1,j-1})], \quad (63)$$

where

$$|\Omega|_{i,j} = 2\Delta S_i \Delta y_j + 2\Delta S_{i-1} \Delta y_{j-1} + \Delta S_i \Delta y_{j-1} + \Delta S_{i-1} \Delta y_j, \quad (64)$$

$$a_{1,i,j} = (y_j S_i^2 + y_{j-1} S_i^2 + y_j S_{i+1}^2) \frac{\Delta y_{j-1}}{\Delta S_i} + (y_j S_i^2 + y_j S_{i+1}^2 + y_{j+1} S_{i+1}^2) \frac{\Delta y_j}{\Delta S_i}, \quad (65)$$

$$a_{2,i,j} = (y_j S_i^2 + y_j S_{i-1}^2 + y_{j-1} S_{i-1}^2) \frac{\Delta y_{j-1}}{\Delta S_{i-1}} + (y_j S_i^2 + y_{j+1} S_i^2 + y_j S_{i-1}^2) \frac{\Delta y_j}{\Delta S_{i-1}}, \quad (66)$$

$$a_{3,i,j} = \rho \theta (y_j S_i + y_{j-1} S_i + y_{j-1} S_{i-1}), \quad (67)$$

$$a_{4,i,j} = \rho \theta (y_j S_i + y_{j-1} S_i + y_j S_{i+1}), \quad (68)$$

$$a_{5,i,j} = \rho \theta (y_j S_i + y_{j+1} S_{i+1} + y_{j+1} S_i), \quad (69)$$

$$a_{6,i,j} = \rho \theta (y_j S_i + y_{j+1} S_i + y_j S_{i-1}), \quad (70)$$

$$a_{7,i,j} = \rho \theta (y_j S_i + y_j S_{i+1} + y_{j+1} S_{i+1}), \quad (71)$$

$$a_{8,i,j} = \rho \theta (y_j S_i + y_j S_{i-1} + y_{j-1} S_{i-1}), \quad (72)$$

$$a_{9,i,j} = \left(r - q - \lambda \kappa (1) - y_j - \frac{1}{2} \rho \theta \right) S_i, \quad (73)$$

$$a_{10,i,j} = \xi (\eta - y_j) - \frac{1}{2} \theta^2 - \frac{1}{2} \rho \theta y_j. \quad (74)$$

In order to satisfy the boundary conditions (49) we set

$$V_{1,j} = 0, \quad V_{N_S,j} = S_{N_S} - E, \quad j = 2, 3, \dots, N_y - 1. \quad (75)$$

Eq. (57) with the substitutions (58)–(63) and the boundary conditions (75) constitute a set of $N_y - 2$ linear systems. More precisely we have one system of N_S equations in the unknowns $V_{1,2}, V_{2,2}, \dots, V_{N_S,2}$, one system of N_S equations in the unknowns $V_{1,3}, V_{2,3}, \dots, V_{N_S,3}$, ..., and one system of N_S equations in the unknowns $V_{1,N_y-1}, V_{2,N_y-1}, \dots, V_{N_S,N_y-1}$. Each one of these systems is in tridiagonal form and hence can be solved very quickly using the well-known algorithm of Thomas; see [46].

Now it remains to compute $V_{i,1}$ and V_{i,N_y} , $i = 1, 2, \dots, N_S$. However, since the partial integro-differential equation (30) is singular at $y = 0$ and $y = +\infty$, it is not clear which boundary conditions to apply at $y = 0$ and $y = y_{\max}$. In this paper, following [24], $V_{i,1}$ and V_{i,N_y} , $i = 2, 3, \dots, N_S - 1$, are obtained by linear extrapolation of the solution on adjacent nodes already computed:

$$V_{i,1} = V_{i,2} - \frac{V_{i,3} - V_{i,2}}{\Delta y_2} \Delta y_1, \quad i = 2, 3, \dots, N_S - 1, \quad (76)$$

$$V_{i,N_y} = V_{i,N_y-1} + \frac{V_{i,N_y-1} - V_{i,N_y-2}}{\Delta y_{N_y-2}} \Delta y_{N_y-1}, \quad i = 2, 3, \dots, N_S - 1. \quad (77)$$

Using relations (76) and (77), in a sense we let the partial integro-differential equation (48) itself impose the boundary conditions at $y = 0$ and $y = y_{\max}$. Finally, according to (49) we set

$$V_{1,j} = 0, \quad V_{N_S,j} = S_{N_S} - E, \quad j = 1, N_y. \quad (78)$$

Now let us solve problem (50)–(51). We multiply Eq. (50) by $\phi_{i,j}(S, y)$ and integrate over $\Omega_{i,j}$, $i = 2, 3, \dots, N_S - 1$, $j = 2, 3, \dots, N_y - 1$. Note that, following the same approach as was used to discretize equation (48), we are only considering

the trial functions centered at the nodes that are internal points of Ω . We obtain

$$\int_{\Omega_{i,j}} W \phi_{i,j} dSdy - \Delta t \int_{\Omega_{i,j}} \mathcal{L}_2 W \phi_{i,j} dSdy = \int_{\Omega_{i,j}} V \phi_{i,j} dSdy, \quad i = 2, 3, \dots, N_S - 1, j = 2, 3, \dots, N_y - 1. \quad (79)$$

Substituting (56) in (79), using relation (34), and applying standard finite element techniques, the integrals appearing at the left hand side of Eq. (79) are approximated as follows:

$$\int_{\Omega_{i,j}} W \phi_{i,j} dSdy \simeq \frac{1}{6} |\Omega|_{i,j} W_{i,j}, \quad (80)$$

$$\int_{\Omega_{i,j}} (\mathcal{L}_2 W) \phi_{i,j} dSdy \simeq \frac{1}{12} [a_{11,i,j}(W_{i,j+1} - W_{i,j}) - a_{12,i,j}(W_{i,j} - W_{i,j-1})], \quad (81)$$

where

$$a_{11,i,j} = \theta^2 \left[(2y_j + y_{j+1}) \frac{\Delta S_{i-1}}{\Delta y_j} + (y_j + 2y_{j+1}) \frac{\Delta S_i}{\Delta y_j} \right], \quad (82)$$

$$a_{12,i,j} = \theta^2 \left[(y_j + 2y_{j-1}) \frac{\Delta S_{i-1}}{\Delta y_{j-1}} + (2y_j + y_{j-1}) \frac{\Delta S_i}{\Delta y_{j-1}} \right]. \quad (83)$$

Moreover the integral appearing in the right hand side of Eq. (79) is computed according to relation (58).

As was done for problem (48)–(49) we use extrapolated boundary conditions at $y = 0$ and $y = y_{\max}$:

$$W_{i,1} = W_{i,2} - \frac{W_{i,3} - W_{i,2}}{\Delta y_2} \Delta y_1, \quad i = 2, 3, \dots, N_S - 1, \quad (84)$$

$$W_{i,N_y} = W_{i,N_y-1} + \frac{W_{i,N_y-1} - W_{i,N_y-2}}{\Delta y_{N_y-1}} \Delta y_{N_y-1}, \quad i = 2, 3, \dots, N_S - 1. \quad (85)$$

Eq. (79), with the substitutions (58), (80), (81), and the boundary conditions (84), (85) constitute a set of $N_S - 2$ linear systems. More precisely we have one system of $N_y - 2$ linear equations in the unknowns $W_{2,2}, W_{2,3}, \dots, W_{2,N_y-1}$, one system of $N_y - 2$ linear equations in the unknowns $W_{3,2}, W_{3,3}, \dots, W_{3,N_y-1}, \dots$, and one system of $N_y - 2$ linear equations in the unknowns $W_{N_S-1,2}, W_{N_S-1,3}, \dots, W_{N_S-1,N_y-1}$. Each one of these systems is in tridiagonal form and is efficiently solved using Thomas's algorithm.

Once the $W_{i,j}, i = 2, 3, \dots, N_S - 1, j = 2, 3, \dots, N_y - 1$, have been obtained, we compute $W_{i,1}$ and W_{i,N_y} using relations (84) and (85), $i = 2, 3, \dots, N_S - 1$. Finally, according to (51), we set

$$W_{1,j} = 0, \quad W_{N_S,j} = S_{N_S} - E, \quad j = 1, 2, \dots, N_y. \quad (86)$$

4.3. Numerical approximation of the integral operator

Let us show how to solve problem (52)–(53). First of all Eq. (52) is collocated at the nodes $(S_i, y_j), i = 2, 3, \dots, N_S - 1, j = 2, 3, \dots, N_y - 1$:

$$\frac{W_{i,j} - U_{i,j}}{\Delta t} + (\mathcal{L}_6 U)_{i,j} = \lambda U_{i,j}, \quad i = 2, 3, \dots, N_S - 1, j = 2, 3, \dots, N_y - 1, \quad (87)$$

where

$$(\mathcal{L}_6 U)_{i,j} = \lambda \int_{-\infty}^{+\infty} U(S_i e^x, y_j) W(dx), \quad i = 2, 3, \dots, N_S - 1, j = 2, 3, \dots, N_y - 1. \quad (88)$$

Moreover, in order to satisfy the boundary conditions (53), we set

$$U_{1,j} = 0, \quad U_{N_S,j} = S_{\max} - E, \quad j = 2, 3, \dots, N_y - 1. \quad (89)$$

Let us define

$$x_{h,i} = \log \left(\frac{S_h}{S_i} \right), \quad h = 2, 3, \dots, N_S, i = 2, 3, \dots, N_S - 1. \quad (90)$$

Using (19) the integral (88) is calculated as follows:

$$(\mathcal{L}_6 U)_{i,j} = \frac{1}{\delta \sqrt{2\pi}} \sum_{h=1}^{N_S} I_{h,i,j}, \quad i = 2, 3, \dots, N_S - 1, j = 2, 3, \dots, N_y - 1, \quad (91)$$

where

$$I_{1,i,j} = \int_{-\infty}^{x_{2,i}} U(S_i e^x, y_j) \exp \left[-\frac{(x - \gamma)^2}{2\delta^2} \right] dx, \quad (92)$$

$$I_{h,i,j} = \int_{x_{h,i}}^{x_{h+1,i}} U(S_i e^x, y_j) \exp \left[-\frac{(x - \gamma)^2}{2\delta^2} \right] dx, \quad h = 2, 3, \dots, N_S - 1, \quad (93)$$

$$I_{N_S,i,j} = \int_{x_{N_S,i}}^{+\infty} U(S_i e^x, y_j) \exp \left[-\frac{(x - \gamma)^2}{2\delta^2} \right] dx. \quad (94)$$

We recall that for $0 \leq S \leq S_{\max}$, $U(S, y_j)$ has been approximated using a piecewise linear function in the S -variable, $j = 1, 2, \dots, N_y$. Moreover for $S > S_{\max}$ we set $U(S, y_j) = S - E, j = 1, 2, \dots, N_y$, so we have for $j = 1, 2, \dots, N_y$,

$$U(S, y_j) = \begin{cases} U_{h,j} + \frac{U_{h+1,j} - U_{h,j}}{\Delta S_h} (S - S_h), & S \in [S_h, S_{h+1}], \quad h = 1, 2, \dots, N_S - 1, \\ S - E, & S \geq S_{\max}. \end{cases} \quad (95)$$

Substituting relations (95) in (92)–(94) and using the fact that, according to (90), $S_i e^{x_{h,i}} = S_h, h = 2, 3, \dots, N_S, i = 2, 3, \dots, N_S - 1$, we obtain

$$I_{1,i,j} \simeq \int_{-\infty}^{x_{2,i}} \left(U_{1,j} + \frac{U_{2,j} - U_{1,j}}{\Delta S_1} S_i e^x \right) \exp \left[-\frac{(x - \gamma)^2}{2\delta^2} \right] dx, \quad (96)$$

$$I_{h,i,j} \simeq \int_{x_{h,i}}^{x_{h+1,i}} \left[U_{1,j} + \frac{U_{h+1,j} - U_{h,j}}{\Delta S_h} S_i (e^x - e^{x_{h,i}}) \right] \exp \left[-\frac{(x - \gamma)^2}{2\delta^2} \right] dx, \quad h = 2, 3, \dots, N_S - 1, \quad (97)$$

$$I_{N_S,i,j} \simeq \int_{x_{N_S,i}}^{+\infty} (S_i e^x - E) \exp \left[-\frac{(x - \gamma)^2}{2\delta^2} \right] dx. \quad (98)$$

Now the integrals (96)–(98) are elementary integrals and can be performed analytically (the calculation is left to the reader). Eq. (87), with the substitutions (91), (96)–(98), and the boundary conditions (89) constitute a set of $N_y - 2$ systems of linear equations. To be precise we have one system of N_S linear equations in the unknowns $U_{1,2}, U_{2,2}, \dots, U_{N_S,2}$, one system of N_S linear equations in the unknowns $U_{1,3}, U_{2,3}, \dots, U_{N_S,3}, \dots$, and one system of N_S linear equations in the unknowns $U_{1,N_y-1}, U_{2,N_y-1}, \dots, U_{N_S,N_y-1}$. Each of these systems has the same matrix, which we term A . It is important to observe that, contrary to what happens for the discretization of the differential operators, where the matrices obtained are tridiagonal, the matrix A is a dense matrix with $N_S \times N_S$ non-zero elements. This reflects the fact that the integral operator \mathcal{L}_6 is a non-local operator, whereas the differential operators $\mathcal{L}_1, \mathcal{L}_2, \dots, \mathcal{L}_5$ are all local operators. However, also despite the fact that A is a dense matrix, an efficient approximation of the integral operator \mathcal{L}_6 is obtained as well, as we are going to explain in the following.

First of all we observe that solving the above $N_y - 2$ linear systems requires us to numerically invert only the matrix A (as the matrix A is common to all the linear systems). Now, the size N_S of the matrix A can be kept reasonably small, as, thanks to the non-uniform mesh, a high level of accuracy can also be reached using a limited number of grid prices. Then, the computer time necessary to invert the matrix A is actually very small (much smaller than the computer time required by the whole simulation). In this respect it is worth noticing that we have obtained $N_y - 2$ linear systems with the same matrix A thanks to the fact that: (1) the jump-integral term has been decoupled from the remaining differential terms using an operator splitting technique; (2) the partial integro-differential problem has been discretized on a finite element mesh of right-angled triangles.

The matrix A is inverted numerically at the beginning of the simulation. Then, at each time step, it is necessary to calculate the product matrix $A^{-1}U$ (here, with abuse of notation, U is used to denote the matrix with entries $U_{i,j}, i = 1, 2, \dots, N_S, j = 2, 3, \dots, N_y - 1$). This amounts to performing, at each time step, $N_S \times N_S \times (N_y - 2)$ floating point operations (i.e. $N_S \times N_S$ floating point operations for each value of $y_j, j = 2, 3, \dots, N_y - 1$), which could seem computationally expensive. However this is not the case. In fact, as already observed, the use of a non-uniform finite element mesh allows us to reach a high level of accuracy also with relatively small values of N_S and N_y (for instance, as shown in Section 5, the choice $N_S = 250$ and $N_y = 200$ gives relative errors of order 10^{-4} or smaller). Then the cost of performing the $N_S \times N_S \times (N_y - 2)$ floating point operations is actually rather moderate in comparison to the accuracy obtained.

Remark 6. As shown in Section 5, if a (non-uniform) finite element mesh of size $N_S = 250, N_y = 200$ is employed (which allows one to obtain relative errors of order 10^{-4} or smaller), then the computer time necessary for evaluating the jump-integral term is roughly half of the computer time required by the whole simulation. That is, the discretization of the non-local integral operator requires about the same time as is necessary for discretizing (all) the other local differential operators. This fact clearly indicates that the numerical approximation of the jump-integral term is performed very efficiently.

Note that the product matrix $A^{-1}U$ could be computed using a fast matrix–matrix multiplication algorithm, which would enhance, to some extent, the speed of the calculation. This approach is followed in [25], where the BLAS optimization library developed by Goto and van de Geijn [47] is employed. Nevertheless, given also that the jump-integral term is already computed quickly (see Remark 6), the advantage of using a fast matrix–matrix multiplication algorithm appears to be small. Thus, for ease of programming, in the present paper such an approach is not employed.

We also observe that the jump-integral term has the form of a correlation product. Then, following, for example [10, 14], [12], [28], we could try to further reduce the cost of evaluating the non-local integral operator by using a numerical integration algorithm based on the fast Fourier transform. In principle, for each $y_j, j = 2, 3, \dots, N_y - 2$, the fast Fourier transform would allow us to compute the jump-integral term with $O(N_S \log_2 N_S)$ floating point operations, against the N_S^2 floating point operations required by the numerical integration technique employed in the present paper. However, as reported in [28], the approach based on the Fourier transform introduces additional localization and interpolation error, especially if it is used in conjunction with a non-uniform spatial mesh, so the discretization of the integral operator must be performed on a price grid which is finer than that employed for the discretization of the differential operators. Moreover the use of the fast Fourier transform requires an iterative solution procedure (unless a fully explicit time stepping is employed), so the calculation of the jump-integral term must be repeated a certain number of times at each time step (roughly three times; see [14]). Therefore, given also that, in practical applications, the mesh-size parameter N_S is limited, for computational reasons, to values of order 10^2 , the advantage of using the fast Fourier transform appears to be small. For this reason, and due to the fact that the jump-integral term is already computed quickly (see Remark 6), in the present paper the fast Fourier transform is not employed. It should also be noted that, up to now, the fast Fourier transform approach has been used for pure jump-diffusion models only, and then it is not exactly clear whether it can be successfully employed for models with both jumps and stochastic volatility (for instance the aforementioned interpolation error might become particularly large in the region where the volatility is small and the solution is less smooth).

The numerical approximation of problem (52)–(53) concludes the k -th step of the cycle (40) and (40)–(44). At this step the approximate values U_{ij}^{k-1} are computed starting from the knowledge of $\Psi_{ij}^k, i = 1, 2, \dots, N_S, j = 1, 2, \dots, N_y$. Once the k -th iteration is performed, then the $(k - 1)$ -th iteration can be started by prescribing, according to relation (43),

$$\Psi_{ij}^{k-1} = \max [U_{ij}^{k-1}, S_i - K], \quad i = 1, 2, \dots, N_S, j = 1, 2, \dots, N_y. \quad (99)$$

Remark 7. A rigorous theoretical analysis concerning the stability and convergence of the numerical method developed in this section appears to be a very difficult task, due to the high complexity level of the partial integro-differential equation (15). In fact such an equation has unbounded variable coefficients, and, as already mentioned, is singular both at $y = 0$ and at $y = +\infty$ (so it is not even clear which boundary conditions to apply at these boundaries). We observe that if the volatility terms were not present in Eq. (15), i.e. if we were dealing with a pure jump-diffusion model, then we would be much better placed. In fact, in such a case, we could make the simple change of variable $x = \log S$ to transform Eq. (15) into an equation with constant coefficients, and then we could exploit well-consolidated techniques (spectral operator techniques, Von Neumann analysis or variational methods; see [44]) to study the convergence properties of the numerical scheme employed. This is done, for example, in [14] and [28], where the stability and the convergence of the numerical method proposed are assessed using the Von Neumann analysis and other related techniques. However, in our case, due to the presence of the volatility terms in Eq. (15), the above techniques cannot be applied. Therefore the convergence properties of the discretization method proposed in this paper are analysed by extensive numerical simulation. This is done in the next section.

Remark 8. In our treatment the two-dimensional unbounded domain is replaced with a bounded one supplied with homogeneous Dirichlet boundary conditions. This is a very common practice in the numerical approximation of partial differential equations defined on unbounded domains. A theoretical analysis of the localization error introduced by this approximation would be as difficult as the problem just mentioned in the previous remark. We just mention the paper by Ehrhardt and Mickens [48], in which this issue is addressed from the analytical standpoint, although in the framework of the (one-dimensional) Black–Scholes model.

5. Numerical results

The simulations are carried out on a computer with a Pentium Dual Core E 2140 Processor 1.6 GHz 2 GB RAM, and the numerical code is written using the Compaq Visual Fortran 6.6 compiler.

The non-uniform finite element mesh is constructed as follows. Along the S -direction we want to have a mesh which is finer in a neighborhood of $S = E$, where the derivative of the payoff function is discontinuous. In contrast, along the y -direction, we want to have a mesh which is finer in a neighborhood of $y = y_0$, where the possible realizations of the variance process are more likely to occur. Therefore, following an approach similar to that employed in [19,30,32], the mesh refinement is done setting

$$S_i = E \left\{ 1 + \frac{1}{\zeta_S} \sinh \left[\frac{i-1}{N_S-1} (c_{2,S} - c_{1,S}) + c_{1,S} \right] \right\}, \quad i = 1, 2, \dots, N_S, \quad (100)$$

Table 1

Comparison between the “true” and the approximate solutions.

Test Case 1.a		
S_0	$C(0, S_0, y_0)$	$C_{ap}(0, S_0, y_0)$
80	1.4843	1.4849
90	3.7145	3.7159
100	7.7027	7.7044
110	13.6722	13.6735
120	21.3653	21.3661
RMSRD = 2.70×10^{-4}		
RUNTIME = 3.8 s		
RUNTIMENOJUMP = 2.2 s		

where

$$c_{1,S} = \operatorname{asinh}(-\zeta_S), \quad c_{2,S} = \operatorname{asinh}\left(\frac{S_{\max} - E}{E} \zeta_S\right), \quad (101)$$

and

$$y_j = y_0 \left\{ 1 + \frac{1}{\zeta_y} \sinh \left[\frac{j-1}{N_y-1} (c_{2,y} - c_{1,y}) + c_{1,y} \right] \right\}, \quad j = 1, 2, \dots, N_y, \quad (102)$$

where

$$c_{1,y} = \operatorname{asinh}(-\zeta_y), \quad c_{2,y} = \operatorname{asinh}\left(\frac{y_{\max} - y_0}{y_0} \zeta_y\right). \quad (103)$$

According to relations (100)–(103) the amount of mesh refinement in the S -direction near $S = E$ is proportional to the parameter ζ_S , whereas the amount of mesh refinement in the y -direction near $y = y_0$ is proportional to the parameter ζ_y (the limit case of $\zeta_S \rightarrow 0$ and $\zeta_y \rightarrow 0$ corresponds to a uniform mesh). In all the simulations presented in this section we use $\zeta_S = 10$ and $\zeta_y = 1$. By means of several numerical experiments we have found that these values allow us to obtain very accurate results.

Test Case 1. For comparison purposes, our first test case is the same test case as is presented in [24]. To be precise, let us consider an American Call option with strike price $E = 100$, maturity $T = 0.5$ year, interest rate $r = 0.03 \text{ year}^{-1}$, and dividend yield $q = 0.05 \text{ year}^{-1}$. The parameters of the Bates model are chosen as follows: $\xi = 2 \text{ year}^{-1}$, $\eta = 0.04 \text{ year}^{-1}$, $\theta = 0.4 \text{ year}^{-1}$, $\lambda = 5 \text{ year}^{-1}$, $\delta = 0.1$, and $\gamma = -\frac{\delta^2}{2}$. As far as the correlation coefficient ρ is concerned, we use both $\rho = 0.5$ (Test Case 1.a) and $\rho = -0.5$ (Test Case 1.b). As was done in [24], for the initial datum S_0 we consider five different values: $S_{0,l} = 80 + 10(l-1)$, $l = 1, 2, 3, 4, 5$. Moreover we set $y_0 = 0.04 \text{ year}^{-1}$.

The mesh-size parameters are chosen as follows: $S_{\max} = 300$, $y_{\max} = 1.0 \text{ year}^{-1}$, $N_S = 250$, $N_y = 200$. Finally we set $N_t = 20$.

Let $C_{ap}(0, S, y)$ denote the approximate value of the American Call option price at time $t = 0$ obtained using the finite element method presented in Section 4. Moreover let RMSRD denote the average relative error on $C_{ap}(0, S, y)$. RMSRD is then computed as follows:

$$\text{RMSRD} = \sqrt{\frac{1}{5} \sum_{l=1}^5 \left(\frac{C_{ap}(0, S_{0,l}, y_0) - C(0, S_{0,l}, y_0)}{C(0, S_{0,l}, y_0)} \right)^2}. \quad (104)$$

Note that accurate estimations of $C(0, S_{0,l}, y_0)$, $l = 1, 2, 3, 4, 5$, necessary for evaluating (104), have been obtained in [24] using a (very time-consuming) finite difference approximation on an extremely fine mesh. Moreover, for test purposes, we denote as RUNTIME the computer time necessary for calculating $C_{ap}(0, S, y)$, and as RUNTIMENOJUMP the computer time necessary for running a simulation in which the discretization of the jump-integral operator is not performed (as if the operator \mathcal{L}_6 was not present in Eq. (31)).

In Tables 1 and 2 we report the values of $C_{ap}(0, S_{0,l}, y_0)$, $C(0, S_{0,l}, y_0)$, $l = 1, 2, 3, 4, 5$, RMSRD, RUNTIME and RUNTIMENOJUMP obtained for Test Case 1.a and Test Case 1.b respectively. Looking at these tables we observe that both in Test Case 1.a and in Test Case 1.b the numerical method proposed in Section 4 is very accurate and fast. In fact the American option price is always computed with at least three correct decimal digits in only 3.8 s. Moreover the relative error RMSRD is very small (of order 10^{-4}). Finally we observe that the computer time RUNTIMENOJUMP is approximately half of the computer time RMSRD. This fact indicates that the discretization of the non-local integral operator is performed very efficiently, as it requires about the same time as is necessary for approximating (all) the other local differential operators.

Comparison with Chiarella et al. [24]. Now let us compare the numerical method proposed in the present paper with that proposed in [24]. In [24] the most significant results obtained in Test Case 1 are the following: in Test Case 1.a the relative

Table 2

Comparison between the “true” and the approximate solutions.

Test Case 1.b		
S_0	$C(0, S_0, y_0)$	$C_{ap}(0, S_0, y_0)$
80	1.1359	1.1356
90	3.3532	3.3537
100	7.5970	7.5986
110	13.8830	13.8852
120	21.7186	21.7209
RMSRD = 1.86×10^{-4}		
RUNTIME = 3.8 s		
RUNTIMENOJUMP = 2.2 s		

Table 3

Comparison between the “true” and the approximate solutions.

Test Case 2		
S_0	$C(0, S_0, y_0)$	$C_{ap}(0, S_0, y_0)$
80	0.328526	0.328446
90	2.109397	2.108750
100	6.711622	6.711854
110	13.749337	13.747836
120	22.143307	22.137798
RMSRD = 2.13×10^{-4}		
RUNTIME = 3.8 s		
RUNTIMENOJUMP = 2.2 s		

error is $\text{RMSRD} = 1.77 \times 10^{-4}$ and the computer time is $\text{RUNTIME} = 12\,120$ s, whereas in Test Case 1.b the relative error is $\text{RMSRD} = 1.93 \times 10^{-4}$ and the computer time is $\text{RUNTIME} = 12\,122$ s. Then, we have: (1) the errors obtained in [24] are approximately equal to those reported in Tables 1 and 2 (actually in Test Case 1.a the error obtained in [24] is slightly smaller, whereas in Test Case 1.b the error obtained in [24] is slightly bigger); (2) the computer times found in [24] are more than a thousand of times bigger than those reported in Tables 1 and 2. It should also be noted that the numerical simulations presented in [24] are carried out on a cluster of computers, which is faster than our Pentium Dual Core processor. Putting all these things together we conclude that in Test Case 1.a and in Test Case 1.b the numerical method proposed in this paper is at least a thousand times faster than the approach followed in [24].

The main reasons why the numerical algorithm developed in this paper is considerably more efficient than the one proposed by [24] are the following: the approach followed in [24] is based on the method of lines, which allows one to reduce the partial integro-differential equation (15) to a system of ordinary differential equations. However, the system of ordinary differential equations obtained is non-linear, and they must be solved using a complex fixed-point iteration method. In particular, to reach convergence, such an iteration procedure requires us to perform, at each time step, a large number of iterations (up to 85 iterations, as reported in [24]), thus reducing the efficiency of the numerical algorithm. Furthermore in [24] a uniform grid is employed, whereas the finite element method proposed in the present paper is carried out on a non-uniform mesh, which, as thoroughly explained in Section 4, is crucial for obtaining an efficient numerical approximation.

Test Case 2. For comparison purposes, as a second test case let us consider the numerical experiment presented in [25]. To be precise let us consider an American Call option with strike price $E = 100$, maturity $T = 0.5$ year, interest rate $r = 0.03 \text{ year}^{-1}$, and dividend yield $q = 0.05 \text{ year}^{-1}$. The parameters of the Bates model are chosen as follows: $\xi = 2 \text{ year}^{-1}$, $\eta = 0.04 \text{ year}^{-1}$, $\theta = 0.25 \text{ year}^{-1}$, $\rho = -0.5$, $\lambda = 0.2 \text{ year}^{-1}$, $\delta = 0.4$, and $\gamma = -0.5$. As was done in Test Case 1, and following also [25], for the initial datum S_0 we consider five different values: $S_{0,l} = 80 + 10(l-1)$, $l = 1, 2, 3, 4, 5$. Moreover we set $y_0 = 0.04 \text{ year}^{-1}$. Finally, as was done in Test Case 1, we set $S_{\max} = 300$, $y_{\max} = 1 \text{ year}^{-1}$, $N_S = 250$, $N_y = 200$, $N_t = 20$ (note that the values of S_{\max} and y_{\max} are the same as those used in [25]). The option price obtained using the numerical method developed in Section 4 is still denoted as $C_{ap}(0, S_0, y_0)$. As was done in Test Case 1, and following also [25], the error on $C_{ap}(0, S_0, y_0)$, which is still denoted as RMSRD, is computed using relation (104). In particular the “true” values of $C(0, S_{0,l}, y_0)$, $l = 1, 2, 3, 4, 5$, necessary for calculating RMSRD are taken from [25], where they have been obtained by performing an accurate (and also very time-consuming) simulation on a very refined mesh.

The results obtained are shown in Table 3 (again we denote as RUNTIME the computer time necessary for obtaining $C_{ap}(0, S_0, y_0)$, and as RUNTIMENOJUMP the computer time necessary for running a simulation in which the discretization of the jump-integral operator is performed). Also in this test case we may note that the numerical method proposed in this paper is very fast and accurate: the American option price is always computed with at least three correct decimal digits in only 3.8 s. As found for Test Case 1, the computer time RUNTIMENOJUMP is approximately half of the computer time RMSRD. This is not surprising, as in Test Case 2 the values used for the mesh-size parameters N_S , N_y , and for the number of time steps N_t are equal to those employed for Test Case 1.

Comparison with Toivanen [25]. Let us compare the numerical method proposed in the present paper with that proposed in [25]. We start by noticing that, as shown in Table 3, the discretization scheme developed in Section 4 allows us to obtain the American option price with relative error $\text{RMSRD} = 2.13 \times 10^{-4}$ in a time $\text{RUNTIME} = 3.8$ s. However, according to what was reported in [25], the numerical method proposed therein allows us to obtain the American option price with relative error $\text{RMSRD} = 3.5 \times 10^{-4}$ in a computer time $\text{RUNTIME} = 109.45$ s. We shall also observe that the simulations presented in [25] are carried out on a computer with a Xeon Processor 3.8 GHz, which has significantly better performance and is faster than our Pentium Dual Core 1.6 GHz processor. Finally, in [25], the product matrix $A^{-1}U$ (see Section 4.3) is evaluated using a fast matrix–matrix multiplication routine (the Goto BLAS optimization library [47]), which is not implemented in our software code. Putting all these things together we conclude that the numerical method proposed in this paper is at least thirty times faster than the method developed in [25].

Let us investigate the reasons why the numerical method proposed in this paper performs significantly better than the method presented in [25]. First of all, in [25] the free boundary problem is solved as a linear complementarity problem, which, as already observed, is rather time-consuming. In contrast, in the present paper, the early exercise feature is taken into account using a faster Richardson extrapolation technique.

More importantly, in [25], some loss of accuracy is also experienced due to the componentwise splitting employed. In fact, such a technique, which is also used in [21] and [22], requires a special treatment of the mixed second-order derivatives, which amounts to changing the coefficients of the diffusive operators in the partial integro-differential equation (15) (see relations (13) in [25]). As a consequence, in the discretized partial integro-differential equation there is added a sort of artificial viscosity, which mars the accuracy of the numerical approximation. However, the operator splitting used in the present paper does not require any special treatment of the mixed second-order derivatives, and hence is computationally more efficient than the componentwise splitting used in [25]. Furthermore the “artificial viscosity” added when using the componentwise splitting depends strongly on the grid stretching (more precisely, the amount of “artificial viscosity” added in the S -direction is directly proportional to the ratio between the distance of two consecutive grid prices and the distance of two consecutive grid variances, whereas the “artificial viscosity” added in the y -direction is directly proportional to the ratio between the distance of two consecutive grid variances and the distance of two consecutive grid prices; see relations (13) in [25]). As shown in [21] and [22], this can compromise the stability of the overall numerical scheme, and imposes severe restrictions on the choice of the grid step sizes when a non-uniform mesh is employed. In this respect it is worth noticing that, according to a numerical test performed by Chiarella et al. in [24], the componentwise splitting employed in [25] “produces prices with some oscillations especially in the negative correlation case” (quoting from [24]).

Finally in [25] a uniform grid is employed, whereas the finite element method proposed in the present paper is carried out on a non-uniform mesh, which, as highlighted in Section 4, is crucial for obtaining an efficient numerical approximation.

Test Case 3. As a third test case we consider an American Put option with strike price $E = 100$, maturity $T = 5$ year, interest rate $r = 0.0319 \text{ year}^{-1}$, and dividend yield $q = 0$. The parameters and data, in common with the Heston model case, are chosen as in [49]: $\xi = 6.21 \text{ year}^{-1}$, $\eta = 0.019 \text{ year}^{-1}$, $\theta = 0.61 \text{ year}^{-1}$, $\rho = -0.7$, $y_0 = 0.010201 \text{ year}^{-1}$. Furthermore we set $\lambda = 0.5 \text{ year}^{-1}$, $\delta = 0.2$, and $\gamma = -\frac{\delta^2}{2}$. Again, for the initial datum S_0 we consider five different values: $S_{0,l} = 80 + 10(l - 1)$, $l = 1, 2, 3, 4, 5$.

The mesh-size parameters S_{\max} , N_S , N_y are chosen as in Test Case 1 and Test Case 2, while $y_{\max} = 0.3$ (the initial variance is significantly smaller than in test Case 1 and Test Case 2), $N_t = 100$ (the option’s maturity is much longer than in Test Case 1 and Test Case 2). Let $P_{ap}(0, S_0, y_0)$ denote the approximate value of the American Put option price obtained using the numerical method proposed in this paper. In order to evaluate the error on $P_{ap}(0, S_0, y_0)$, an estimation of the true American Put option price, denoted as $P(0, S_0, y_0)$, is obtained by performing a very accurate (and also very expensive) simulation with the following mesh-size parameters: $S_{\max} = 450$, $y_{\max} = 0.45 \text{ year}^{-1}$, $N_S = 500$, $N_y = 500$, $N_t = 400$. As was done in Test Case 1 and in Test Case 2, the average relative error on $P_{ap}(0, S_0, y_0)$, which is still denoted as RMSRD , is computed using relation (104) in which $C(0, S_0, y_0)$ and $C_{ap}(0, S_0, y_0)$ are replaced with $P(0, S_0, y_0)$ and $P_{ap}(0, S_0, y_0)$. Again, we denote as RUNTIME the computer time necessary for obtaining $P_{ap}(0, S_0, y_0)$, as RUNTIMENOJUMP the computer time necessary for running a simulation in which the discretization of the jump-integral operator is performed. In Table 4 we show the values of $P_{ap}(0, S_{0,l}, y_0)$, $P(0, S_{0,l}, y_0)$, $l = 1, 2, 3, 4, 5$, RMSRD , RUNTIME and RUNTIMENOJUMP found in Test Case 3. We may note that the numerical method proposed in this paper is very accurate and fast. In fact the American option price is always computed with at least four correct decimal digits (average relative error of order 10^{-5}) in only 16.3 s. Moreover, as happens in Test Case 1 and Test Case 2, the computer time RUNTIMENOJUMP is about half of the computer time RUNTIME , which indicates that also in Test Case 3 the numerical approximation of the non-local integral operator has been performed efficiently.

Finally we note that in Test Case 3 the initial datum y_0 is a very small value. In addition we have $\theta^2 > 2\xi\eta$, so the variance process is allowed to hit the origin. As a consequence the realizations of Y_t are contained with probability close to 1 in a region close to $y = 0$, where the partial integro-differential equation (15) is singular. Also despite this fact the numerical method proposed in this paper allows us to obtain very accurate results.

Computing the early exercise boundary and the hedge parameters. Starting from the finite element solution obtained, we can evaluate the early exercise boundary and the hedge parameters Δ and Γ , that is the first-order and the second-order derivatives of the option price with respect to the underlying asset price. Let us now show how. For the sake of brevity, these quantities are computed at time $t_0 = 0$; however the calculation for times greater than zero is identical.

Table 4

Comparison between the “true” and the approximate solutions.

Test Case 3		
S_0	$P(0, S_0, y_0)$	$P_{ap}(0, S_0, y_0)$
80	21.3053	21.3030
90	15.6365	15.6364
100	11.5887	11.5890
110	8.6680	8.6685
120	6.5464	6.5466
RMSRD = 5.77×10^{-5}		
RUNTIME = 16.3 s		
RUNTIMENOJUMP = 7.5 s		

Table 5

Early exercise boundary and hedge parameters.

Test Case 1.a				
$S_b = 138.771, S_{b,ap} = 138.887$				
S_0	Δ	Δ_{ap}	Γ	Γ_{ap}
80	0.152074	0.152074	0.012178	0.012177
90	0.303638	0.303538	0.017853	0.017883
100	0.498102	0.498002	0.020256	0.020262
110	0.690994	0.690967	0.017480	0.017483
120	0.838096	0.838085	0.011928	0.011928
$ERR_{S_b} = 8.36 \times 10^{-4}, RMSRD_{\Delta} = 1.75 \times 10^{-4}, RMSRD_{\Gamma} = 7.55 \times 10^{-4}$				

For ease of exposition, we focus our attention on an American option of Call type (for the American Put the procedure is analogous). Moreover, following the notation used previously, the finite element approximation of the option price at time zero is denoted as $C_{ap}(0, S, y_0)$.

According to relation (21), the early exercise boundary is obtained as the point at which the function $C_{ap}(0, S, y_0)$ intersects the function $\max[S - K, 0]$. This intersection is readily obtained, as both $C_{ap}(0, S, y_0)$ and $\max[S - K, 0]$ are piecewise linear functions.

Instead, in order to compute the parameters Δ and Γ , we shall use an interpolation procedure, as the derivatives of the function $C_{ap}(0, S, y_0)$ with respect to S are not continuous. Therefore, let S_{i_0} denote the node of the mesh such that $S_{i_0} \leq S_0 < S_{i_0+1}$ (i.e. the initial price S_0 lies between the price nodes S_{i_0} and S_{i_0+1}). To compute Δ and Γ we use the cubic polynomial that interpolates the function $C_{ap}(0, S, y_0)$, along the S -variable, at the four grid points $S_{i_0-1}, S_{i_0}, S_{i_0+1}, S_{i_0+2}$. To be precise, the parameters Δ and Γ are obtained as the first-order and the second-order derivatives of this polynomial at $S = S_0$, respectively.

Note that the above approach for calculating the free boundary and the hedge parameters is a simple postprocessing of the solution obtained by finite element approximation. Therefore the computer time necessary for evaluating these quantities is just an offset of the computer time necessary for obtaining the American option price.

Using the above procedure, we compute the values of the early exercise boundary and the hedge parameters in Test Case 1, Test Case 2, and Test Case 3. Moreover we estimate the errors obtained by comparison with “true” values of the free boundary and of Δ and Γ , which are computed by applying the above postprocessing procedure to very accurate finite element solutions. To be precise, in Test Case 1 and Test Case 2 these very accurate solutions are obtained by running the finite element method with the following mesh-size parameters: $S_{\max} = 450, y_{\max} = 1.5 \text{ year}^{-1}, N_S = 500, N_y = 500, N_t = 400$. Instead, in Test Case 3 we employ the same very accurate solution as we already used to estimate the error on the finite element approximation $P_{ap}(0, S_{0,i}, y_0)$.

The results obtained in Test Case 1.a, Test Case 1.b, Test Case 2, and Test Case 3 are reported in Table 5, Table 6, Table 7, Table 8, respectively. In these tables $S_{b,ap}$ denotes the value of the early exercise boundary obtained using the finite element method, S_b denotes the “true” value of the early exercise boundary, and ERR_{S_b} denotes the relative error on $S_{b,ap}$ ($ERR_{S_b} = |S_{b,ap} - S_b| / S_b$). Furthermore Δ_{ap} and Γ_{ap} denote the approximate values of Δ and Γ , respectively. Finally the errors on Δ and Γ , which are denoted by $RMSRD_{\Delta}$ and $RMSRD_{\Gamma}$, are calculated using relations analogous to (104).

Looking at Tables 5–8 we may observe that the method proposed in this paper allows us to obtain a very satisfactory approximation of the free boundary and of the hedge parameters, which are always computed with errors of order 10^{-4} . Again in Test Case 1.a and Test Case 1.b we can make a comparison with the method of lines used by Chiarella et al., as in [24] there are also reported the errors and the computer times relating to the calculation of Δ and Γ (see Figure 8 and Figure 9 in [24]). Now, using the method developed in the present paper, for Test Case 1.a and Test Case 1.b the parameters Δ and Γ are computed with errors of order 10^{-4} in 3.8 s (this computer time was shown in Tables 1 and 2). Instead, using the method of lines of [24], the computer times required to evaluate Δ and Γ with an error of order 10^{-4} are of order 10^2 s or 10^3 s

Table 6

Early exercise boundary and hedge parameters.

Test Case 1.b				
$S_b = 147.800, S_{b,ap} = 147.918$				
S_0	Δ	Δ_{ap}	Γ	Γ_{ap}
80	0.140008	0.140013	0.013604	0.013605
90	0.316095	0.316104	0.020954	0.020947
100	0.532529	0.533042	0.020856	0.020823
110	0.715582	0.715586	0.015465	0.015465
120	0.842646	0.842633	0.010158	0.010158
$ERR_{S_b} = 7.98 \times 10^{-4}, RMSRD_{\Delta} = 4.31 \times 10^{-4}, RMSRD_{\Gamma} = 7.40 \times 10^{-4}$				

Table 7

Early exercise boundary and hedge parameters.

Test Case 2				
$S_b = 163.066, S_{b,ap} = 163.216$				
S_0	Δ	Δ_{ap}	Γ	Γ_{ap}
80	0.073208	0.073208	0.014376	0.014373
90	0.310482	0.310563	0.030304	0.030335
100	0.600090	0.600288	0.024766	0.024790
110	0.787351	0.787364	0.013110	0.013111
120	0.878950	0.878961	0.006087	0.006089
$ERR_{S_b} = 9.17 \times 10^{-4}, RMSRD_{\Delta} = 1.89 \times 10^{-4}, RMSRD_{\Gamma} = 6.70 \times 10^{-4}$				

Table 8

Early exercise boundary and hedge parameters.

Test Case 3				
$S_b = 73.873, S_{b,ap} = 73.904$				
S_0	Δ	Δ_{ap}	Γ	Γ_{ap}
80	−0.674027	−0.673717	0.025978	0.025931
90	−0.475380	−0.475317	0.015868	0.015859
100	−0.341924	−0.3419247	0.011153	0.011149
110	−0.247551	−0.247586	0.007909	0.007907
120	−0.180566	−0.180620	0.005621	0.005620
$ERR_{S_b} = 4.20 \times 10^{-4}, RMSRD_{\Delta} = 2.61 \times 10^{-4}, RMSRD_{\Gamma} = 8.88 \times 10^{-4}$				

(we recall that the simulations presented in [24] are carried out on a computer which is more powerful than our Pentium Dual Core processor). Therefore, also for the calculation of the hedge parameters Δ and Γ , the finite element method developed in this paper performs significantly better than the approach proposed in [24].

6. Conclusions

A finite element method for pricing American options on an underlying described by the Bates model is proposed. In particular, it is shown how relatively simple tools (Richardson extrapolation, implicit/explicit time stepping, operator splitting, non-uniform finite element mesh), if appropriately combined together, allow us to obtain a highly efficient numerical method for this kind of problem. In fact, in all the numerical simulations performed, relative errors of order 10^{-4} or smaller are obtained in a time equal to or smaller than 16.3 s (using a computer with a Pentium Dual Core E 2140 Processor 1.6 GHz 2 GB RAM). Moreover, the discretization of the non-local integral operator is performed efficiently, as it requires about the same computer time as is necessary to discretize (all) the other local operators in the partial integro-differential equation. It is also worth noticing that excellent results are also obtained when the variance process is extremely close the origin, or when the option's maturity is long.

Although a rigorous theoretical analysis of the method proposed has not been performed, due to the high complexity level of the partial integro-differential equation arising in the Bates model, the reasons why such a level of computational efficiency is reached are shown and discussed in detail. In particular, it is clearly explained why the numerical algorithm presented in the present paper performs significantly better than other methods that have been recently proposed for pricing American options under the Bates model.

Finally it is worth noticing that the numerical strategy developed in this paper could also be used for the pricing of other kinds of derivatives, such as barrier options and more exotic products.

References

- [1] F. Black, M. Scholes, The pricing of options and corporate liabilities, *J. Political Economy* 81 (1973) 637–659.
- [2] R. Cont, P. Tankov, *Financial Modelling with Jumps*, Chapman/Hall-CRC, 2004.
- [3] O.E. Barndorff-Nielsen, N. Shephard, Ornstein–Uhlenbeck-based models and some of their uses in financial economics (with discussion), *J. R. Stat. Soc. B* 63 (2001) 167–241.
- [4] O.E. Barndorff-Nielsen, N. Shephard, Modelling by Lévy processes for financial econometrics, in: O. Barndorff-Nielsen, T. Mikosch, S. Resnick (Eds.), *Lévy Processes—Theory and Applications*, Birkhäuser, 2001, pp. 283–318.
- [5] D. Bates, Jumps and stochastic volatility: the exchange rate processes implicit in Deutschmark options, *Rev. Fin. Studies* 9 (1996) 69–107.
- [6] P. Carr, E. Geman, D. Madan, M. Yor, Stochastic volatility for Lévy processes, *Math. Finance* 13 (2003) 345–382.
- [7] R. Merton, Option pricing when underlying stock returns are discontinuous, *J. Fin. Economics* 3 (1976) 125–144.
- [8] S.L. Heston, A closed-form solution for options with stochastic volatility with applications to bond and currency options, *Rev. Fin. Studies* 6 (1993) 327–343.
- [9] A.M. Matache, P.A. Nitsche, C. Schwab, Wavelet Galerkin pricing of American options on Lévy driven assets, *Quant. Finance* 5 (2005) 403–424.
- [10] L. Andersen, J. Andreasen, Jump-diffusion processes: volatility smile fitting and numerical methods for pricing, *Rev. Derivatives Res.* 4 (2000) 231–262.
- [11] R. Cont, E. Voltchkova, A finite difference scheme for option pricing in jump-diffusion and exponential levy models, *SIAM J. Numer. Anal.* 43 (2005) 1596–1626.
- [12] Y. d'Halluin, P.A. Forsyth, G. Labahn, A penalty method for American options with jump diffusion processes, *Num. Math.* 97 (2004) 321–352.
- [13] P.A. Forsyth, K.R. Vetzal, R. Zvan, A penalty method for American options with stochastic volatility, *J. Comput. Appl. Math.* 91 (1998) 199–218.
- [14] S.S. Clift, P.A. Forsyth, Numerical solution of two asset jump diffusion models for option valuation, *Appl. Numer. Math.* 58 (2008) 743–782.
- [15] F. Fang, C.W. Oosterlee, A novel option pricing method based on Fourier–cosine series expansions, *SIAM J. Sci. Comput.* 31 (2008) 826–848.
- [16] F. Fang, C.W. Oosterlee, Pricing early-exercise and discrete barrier options by Fourier–cosine series expansions, *Numer. Math.* 114 (2009) 27–62.
- [17] Y. Achdou, N. Tchou, Variational analysis for the Black–Scholes equation with stochastic volatility, *ESAIM: Mat. Mod. Num. Anal.* 36 (2002) 373–395.
- [18] N. Hilber, A.-M. Matache, C. Schwab, Sparse wavelet methods for option pricing under stochastic volatility, *J. Comput. Finance* 8 (2005) 1–42.
- [19] N. Clarke, K. Parrot, Multigrid for American option pricing with stochastic volatility, *Appl. Math. Finance* 6 (1999) 177–195.
- [20] S. Ikonen, J. Toivanen, Operator splitting methods for American option pricing, *Appl. Math. Lett.* 17 (2004) 809–814.
- [21] S. Ikonen, J. Toivanen, Componentwise splitting methods for pricing American options under stochastic volatility, *Int. J. Theor. Appl. Fin.* 10 (2007) 331–361.
- [22] S. Ikonen, J. Toivanen, Efficient numerical methods for pricing American options under stochastic volatility, *Numer. Methods Partial Differential Equations* 24 (2008) 104–126.
- [23] E. Miglio, C. Sgarra, A finite element framework for option pricing with the bates model, Preprint. Presented at the 3rd AMAMEF Conference, Vienna, 17–22 September 2007.
- [24] C. Chiarella, B. Kang, G.H. Meyer, A. Zogas, The evaluation of American option prices under stochastic volatility and jump-diffusion dynamics using the method of lines, *Int. J. Theor. Appl. Finance* 12 (2009) 393–425.
- [25] J. Toivanen, A componentwise splitting method for pricing American options under the Bates model, in: W. Fitzgibbon, Yu. Kuznetsov, P. Neittaanmäki, J. Periaux, O. Pironneau (Eds.), *Applied and Numerical Partial Differential Equations: Scientific Computing, Simulation, Optimization and Control in a Multidisciplinary Context*, in: *Computational Methods in Applied Sciences*, vol. 15, Springer, 2010, pp. 213–227.
- [26] G. Cheang, C. Chiarella, A. Zogas, The representation of American options prices under stochastic volatility and jump-diffusion dynamics, in: *Research Paper Series*, vol. 256, Quantitative Finance Research Centre, University of Technology, Sydney, 2009.
- [27] P. Carr, D. Madan, Option valuation using the fast Fourier transform, *J. Comput. Finance* 2 (1998) 61–73.
- [28] Y. d'Halluin, P.A. Forsyth, K.R. Vetzal, Robust numerical methods for contingent claims under jump diffusion processes, *IMA J. Numer. Anal.* 25 (2005) 87–112.
- [29] M.J. Brennan, E.S. Schwartz, The Valuation of American Put Options, *J. Finance* 32 (1977) 449–462.
- [30] K. Itô, J. Toivanen, Lagrange multiplier approach with optimized finite difference stencils for pricing American options under stochastic volatility, *SIAM J. Sci. Comp.* 31 (2009) 2646–2664.
- [31] P.A. Forsyth, K.R. Vetzal, Quadratic convergence for valuing American options using a penalty method, *SIAM J. Sci. Comput.* 23 (2002) 2095–2122.
- [32] C.W. Oosterlee, C.C.W. Leentvaar, X. Huang, Accurate American option pricing by grid stretching and high order finite differences, Preprint, Delft Inst. of Applied Mathematics (2009).
- [33] J.C. Cox, J.E. Ingersoll, S.A. Ross, A theory of the term structure of interest rates, *Econometrica* 53 (1985) 385–407.
- [34] W. Feller, Two singular diffusion problems, *Ann. Math.* 54 (1951) 173–182.
- [35] K. Sato, *Lévy Processes and Infinitely Divisible Distributions*, Cambridge University Press, 1999.
- [36] J. Jacod, A.N. Shiryaev, *Limit Theorems for Stochastic Processes*, 2nd ed., Springer, 2002.
- [37] D. Sevcovic, Transformation methods for evaluating approximations to the optimal exercise boundary for linear and nonlinear Black–Scholes equations, in: *Nonlinear Models in Mathematical Finance: New Research Trends in Option Pricing*, Nova Science Publishers, Hauppauge, NY, 2008, pp. 153–198.
- [38] R. Lord, F. Fang, F. Bervoets, C.W. Oosterlee, A fast and accurate FFT-based method for pricing early-exercise options under levy processes, *SIAM J. Sci. Comput.* 30 (2008) 1678–1705.
- [39] S.L. Chung, C.C. Chang, R.C. Stapleton, Richardson extrapolation techniques for the pricing of American-style options, *J. Futures Markets* 27 (2007) 791–817.
- [40] D.W. Peaceman, H.H. Rachford, The numerical solution of parabolic and elliptic differential equations, *J. Soc. Ind. Appl. Math.* 3 (1955) 28–41.
- [41] S. McKee, D.P. Wall, S.K. Wilson, An alternating direction implicit scheme for parabolic equations with mixed derivative and convective terms, *J. Comput. Phys.* 126 (1996) 64–76.
- [42] W.H. Hundsdorfer, J.G. Verwer, *Numerical Solution of Time-Dependent Advection–Diffusion–Reaction Equations*, Springer, 2003.
- [43] C. Hirsch, *Numerical Computation of Internal and External Flows*, Vol. 1 – Fundamentals of Numerical Discretization, Wiley, 1988.
- [44] A. Quarteroni, A. Valli, *Numerical Approximation of Partial Differential Equations*, Springer-Verlag, 1994.
- [45] G. Strang, G. Fix, *An Analysis of the Finite Element Method*, Prentice-Hall, 1973.
- [46] L.H. Thomas, Elliptic problems in linear difference equations over a network, *Watson Sci. Comput. Lab. Report*, Columbia University, New York, 1949.
- [47] K. Goto, R.A. van de Geijn, Anatomy of high-performance matrix multiplication, *ACM Trans. Math. Software* 34 (12) (2008) 25.
- [48] M. Ehrhardt, R.E. Mickens, A fast, stable and accurate numerical method for the Black–Scholes equation of American options, *Int. J. Theor. Appl. Finance* 11 (2008) 471–501.
- [49] M. Broadie, Ö. Kaya, Exact simulation of stochastic volatility and other affine jump diffusion processes, *Oper. Res.* 54 (2006) 217–231.